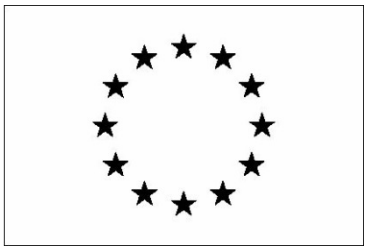

Grant Agreement number: **248095**

Project acronym: **Q-ESSENCE**

Project title: **Quantum Interfaces, Sensors, and Communication based on Entanglement**

Funding Scheme: **Collaborative Project (Large-Scale Integrating Project)**

DELIVERABLE REPORT

Deliverable no.:	**D1.1.4**
Deliverable name:	***Report on quantum vs. classical scaling of phase estimation precision in the presence of losses***
Workpackage no.	**WP1.1**
Lead beneficiary	**UWAW**
Nature	**R = Report**
Dissemination level	**PU = Public**
Delivery date from Annex I (proj month)	**31/01/2013**
Actual / forecast delivery date	**31/01/2013**
Status	**Submitted**

D1.1.4
Report on quantum vs. classical scaling of phase estimation precision in the presence of losses

In [DGK1-12] general tools have been developed that allow for an efficient calculation of fundamental bounds on precision of quantum phase estimation in the presence of general decoherence models, in particular loss. The two methods are based on geometry of quantum channels (classical simulation method, CS) and semi-definite programming (channel extension method, CE). Thinking of parameter estimation as a problem of determining movement of a channel in the space of quantum channels, CS method amounts to a study of the distance of a given channel to the boundary of the set of quantum channels along the tangent to its trajectory. This method allows to get a useful bounds for models in which these distance is non-zero as is the case e.g. in the dephasing and depolarization models. This is not possible, however, when loss is the only source of decoherence. In this case the channel lays on the boundary of the set of quantum channels and the tangent to its trajectory sticks out of the set of quantum channels making the distances used in the formula for the fundamental bounds zero. Fortunately, the CE method is capable of dealing with this model and allows to derive a useful bound, which is moreover saturable in the asymptotic limit of large number of probes by a simple strategy based on mixing coherent and squeezed vacuum state on a beam splitter. Figure 1 below depicts models to which the tools have been applied and Table 1 shows the corresponding bounds derived using the two methods.

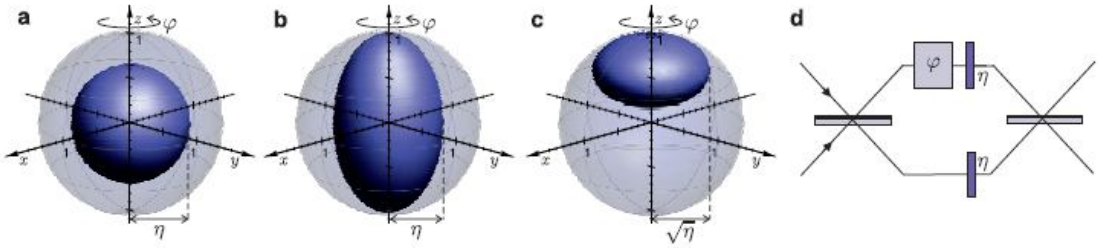

Figure 1 Graphical representation of some of the most relevant models for decoherence In the context of quantum metrology. (a) Qubit depolarization (b) Qubit dephasing (c) Spontaneous emission (d) Lossy interferometer. In all models η is the decoherence parameter, where η=1 corresponds to no decoherence and η=0 corresponds to the complete loss of coherence.

Model	Depolarization	Dephasing	Spontaneous emission	Loss
$\Delta\varphi_{\mathrm{CS}}$	$\sqrt{\frac{(1-\eta)(1+3\eta)}{4\eta^2 n}}$	$\sqrt{\frac{1-\eta^2}{\eta^2 n}}$	-	-
$\Delta\varphi_{\mathrm{CE}}$	$\sqrt{\frac{(1-\eta)(1+2\eta)}{2\eta^2 n}}$	$\sqrt{\frac{1-\eta^2}{\eta^2 n}}$	$\sqrt{\frac{1-\eta}{4\eta n}}$	$\sqrt{\frac{1-\eta}{\eta n}}$

Table 1 Lower bounds on minimum uncertainty of phase estimation for different decoherence models calculated with the help of the two methods: classical simulation (CS) and channel extension (CE) as a function of decoherence parameter η and the number of probes (qubits, photons) used. In particular CE method allows to derive a saturable bound for the asymptotic scaling (large n) of precision under loss.

These results clearly show that in the asymptotic regime there is no possibility for the Heisenberg like scaling and the quantum enhancement has a constant factor improvement character rather than providing a better scaling of precision with increasing number of probes. More precisely in the case of loss the asymptotic gain in precision is equal to $(1-\eta)^{1/2}$ where η is the power transmission coefficient in the interferometer.

Moreover in [KD1-13] we have also generalized the CE method to provide tighter bounds in the regime of finite number of probes. We have also analyzed the quantum simulation (QS) method, and showed that it is a special case of the CE method. In particular, we have showed that QS method is sufficient to derive bounds for phase estimation with loss asymptotically equivalent to the ones derived with the help of the CE method.

[DGK1-12] R. Demkowicz-Dobrzanski, M. Guta, J. Kolodynski, *The elusive Heisenberg limit in quantum enhanced metrology*, Nature Communications **3**, 1063 (2012)

[KD1-13] J. Kolodynski, R. Demkowicz-Dobrzanski, *Efficient tools for quantum metrology with uncorrelated noise* (2013) arXiv:1303.7271, to appear in New J. Phys.

nature COMMUNICATIONS

OPEN

ARTICLE

Received 16 Apr 2012 | Accepted 14 Aug 2012 | Published 18 Sep 2012

DOI: 10.1038/ncomms2067

The elusive Heisenberg limit in quantum-enhanced metrology

Rafał Demkowicz-Dobrzański[1], Jan Kołodyński[1] & Mădălin Guță[2]

Quantum precision enhancement is of fundamental importance for the development of advanced metrological optical experiments, such as gravitational wave detection and frequency calibration with atomic clocks. Precision in these experiments is strongly limited by the $1/\sqrt{N}$ shot noise factor with N being the number of probes (photons, atoms) employed in the experiment. Quantum theory provides tools to overcome the bound by using entangled probes. In an idealized scenario this gives rise to the Heisenberg scaling of precision $1/N$. Here we show that when decoherence is taken into account, the maximal possible quantum enhancement in the asymptotic limit of infinite N amounts generically to a constant factor rather than quadratic improvement. We provide efficient and intuitive tools for deriving the bounds based on the geometry of quantum channels and semi-definite programming. We apply these tools to derive bounds for models of decoherence relevant for metrological applications including: depolarization, dephasing, spontaneous emission and photon loss.

[1] Faculty of Physics, University of Warsaw, ul. Hoża 69, PL-00-681 Warszawa, Poland. [2] School of Mathematical Sciences, University of Nottingham, University Park, NG7 2RD Nottingham, UK. Correspondence and requests for materials should be addressed to R.D.-D. (email: demko@fuw.edu.pl).

Quantum-enhanced metrology aims to exploit quantum features of atoms and light such as entanglement, for measuring physical quantities with precision going beyond the classical limit[1–4]. A prominent example is that of an optical interferometer, where interference of photons at the output port carries information on the relative optical path difference between the interferometer arms. When standard laser light is used, the observed results are compatible with the claim that 'each photon interferes only with itself'[5] and the whole process may be regarded as sensing with N independent probes (photons). Parameter estimation with N independent probes yields the $1/\sqrt{N}$ 'standard scaling' (SS) of precision[6]. Entangling the probes however, can in principle offer a quadratic enhancement in precision, that is, the $1/N$ or 'Heisenberg scaling' (HS)[7–11]. Such strategies have been experimentally realized in optical interferometry[12–16] with exciting applications in the quest for the first direct detection of gravitational waves[17,18]. Moreover, the same quantum enhancement principle can be utilized in atomic spectroscopy[19,20] where the spin-squeezed states have been employed for improving frequency calibration precision[21–24]. Alternative approaches to beat the SS without resorting to quantum entanglement include multiple-pass[25,26] and non-linear metrology[27,28].

Unfortunately, both the theory[29–35] and experiments[36,37] confirmed the fragility of the above schemes when noise sources such as decoherence are considered, and it has been rigorously shown for particular models that asymptotically with respect to N, even infinitesimally small noise turns HS into SS, so that the quantum gain amounts to a constant factor improvement[38–40].

In this paper, we develop two methods that allow us to extend these partial results to a broad class of decoherence models, and in particular to obtain fundamental bounds on quantum enhancement for the most relevant models encountered in the quantum metrology literature. The two approaches complement each other in terms of provided intuition and power. The first method elaborates on the idea of 'classical simulation' (CS)[41] and provides a bound based solely on the geometry of the space of quantum channels (SQC). When applicable, it gives an excellent intuition as to why the HS is lost in the presence of decoherence, but fails to yield useful bounds for some relevant decoherence models. The second method is based on the 'channel extension' (CE) strategy[42] and requires the optimization over different Kraus representation of a quantum channel. However, unlike the earlier work[40], which involved making an educated guess about the appropriate class of Kraus representations, our bound can be cast into an explicit semi-definite optimization problem, which is easy to solve even for complex models. The power of the method is demonstrated by obtaining new bounds for depolarization and spontaneous emission models, and re-deriving asymptotic bounds for dephasing and lossy interferometer with unprecedented simplicity.

Results

Bounds on precision in quantum-enhanced metrology. The typical quantum metrology scenario is depicted in Fig. 1a. An ensemble of N quantum systems undergo in parallel the same transformation Λ_φ, which depends on an unknown physical parameter φ. The output state is measured and the outcome is used to compute an estimate $\tilde{\varphi}$ of the parameter φ as summarized below

$$\varphi \to \Lambda_\varphi^{\otimes N}\left[\rho^N\right] \to \tilde{\varphi}. \tag{1}$$

The task is to find the optimal (possibly highly entangled) input state ρ^N and the most effective measurement strategy to minimize the estimation error $\Delta\varphi_N$. Note that since the decoherence process is assumed to act independently on each of the probes, the global channel is described by the tensor product $\Lambda_\varphi^{\otimes N}$.

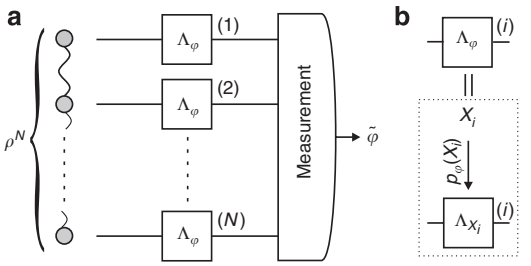

Figure 1 | Quantum metrology and the CS idea. (**a**) General scheme for quantum-enhanced metrology. N-probe quantum state fed into N parallel channels is sensing an unknown channel parameter φ. An estimator $\tilde{\varphi}$ is inferred from a measurement result on the output state. (**b**) CS of a quantum channel. The channel Λ_φ is interpreted as a mixture of other channels Λ_X, where the dependence on φ is moved into the mixing probabilities $p_\varphi(X)$.

We pursue the estimation problem by restricting our attention to estimators, which are unbiased in the neighbourhood of some fixed parameter value, for which the quantum Cramér–Rao bound (CRB) holds

$$\Delta\varphi_N \geq \frac{1}{\sqrt{F_Q\left[\Lambda_\varphi^{\otimes N}\left[\rho^N\right]\right]}}, \tag{2}$$

where F_Q is the quantum Fisher information (QFI)[9]. Maximization of QFI over input states ρ^N sets the limit on the achievable quantum-enhanced precision:

$$\Delta\varphi_N \geq \frac{1}{\sqrt{\mathcal{F}_N}}, \quad \mathcal{F}_N = \max_{\rho^N} F_Q\left[\Lambda_\varphi^{\otimes N}\left[\rho^N\right]\right]. \tag{3}$$

The states that maximize the QFI and yield the HS for decoherence-free unitary channels are typically highly entangled: the GHZ state in the case of atomic spectroscopy[43], and the N00N state in the case of optical interferometry[44]. In the presence of decoherence, the optimal input states do not have an intuitive form and the maximization of the QFI (with rising N) becomes hard even numerically[20,29,30].

The typical behaviour of the estimation uncertainty in the presence of decoherence is depicted in the log–log scale in Fig. 2, showing that asymptotically in N the quantum gain amounts to a constant factor improvement over the standard $1/\sqrt{N}$ scaling achievable with independent probes. The key result of this paper is to provide a method for a general and simple calculation of this constant factor improvement.

Classical simulation. To understand the idea of CS, we need to think of quantum channels in a geometrical way[45]. A quantum channel is a completely positive, trace-preserving map acting on density matrices. The space of all such transformations is convex: if Λ, Λ' are two channels, then $p\Lambda + (1-p)\Lambda'$ can be realised by randomly applying Λ or Λ' with probabilities p and $1-p$. The channels that cannot be decomposed into a convex combination of different channels (for example, the unitary transformations) are called 'extremal'. Note that while all interior points of the SQC are 'non-extremal', the boundary contains both the extremal as well as some non-extremal channels.

We say that the family Λ_φ is 'classically simulated'[41] if each channel is written as a classical mixture of the form

$$\Lambda_\varphi[\rho] = \int \mathrm{d}x \; p_\varphi(x)\, \Lambda_x[\rho], \tag{4}$$

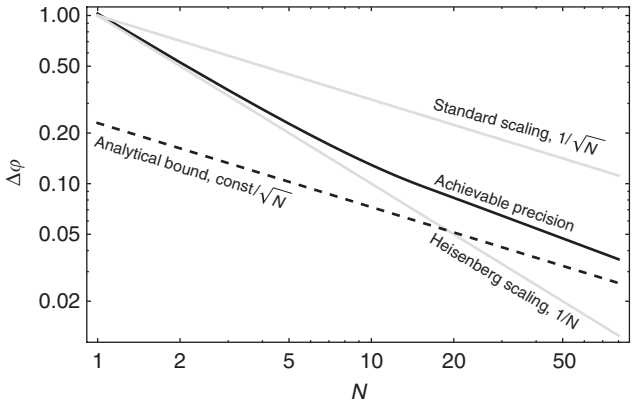

Figure 2 | Estimation precision in presence of decoherence. Log–log plot of a generic dependence of quantum-enhanced parameter estimation uncertainty in the presence of decoherence as a function of the number of probes used. While for small number of probes the curve for achievable precision follows the Heisenberg scaling, it asymptotically flattens to approach const/$\sqrt{N}$ dependence. The 'const' represents the quantum enhancement factor. The exemplary data corresponds to the case of phase estimation using N photons in a Mach–Zehnder interferometer with 5% losses in both arms.

where the unknown parameter enters only through the probability distribution p_φ of a random variable X that indicates which channel to pick from the set $\{\Lambda_x\}$ (Fig. 1b). If $X_1,\ldots,X_N$ are the independent hidden random variables used to generate the parallel channels, we can rewrite the estimation problem as

$$\varphi \to \{X_i\}_{i=1}^N \to \otimes_{i=1}^N \Lambda_{X_i}\left[\rho^N\right] \to \tilde{\varphi}. \tag{5}$$

Since conditionally on the values of X_i the output state does not carry any information about φ, the estimation precision in the above scenario is at most equal to that of the classical problem of estimating φ given N independent samples from the distribution p_φ

$$\varphi \to \{X_i\}_{i=1}^N \to \tilde{\varphi}. \tag{6}$$

Hence, using the classical CRB[46], we obtain a lower bound on the uncertainty of the original problem equation (1)

$$\Delta\varphi_N \geq \frac{1}{\sqrt{N\,F_{\rm cl}[p_\varphi]}},\quad F_{\rm cl} = \int dx \frac{\left[\partial_\varphi p_\varphi(x)\right]^2}{p_\varphi(x)}, \tag{7}$$

where $F_{\rm cl}$ is the classical Fisher information; see Methods for an alternative derivation.

Provided that $p_\varphi(x)$ satisfies regularity conditions required in the derivation of CRB[46], the SS of precision follows immediately. Moreover, any particular CS yields an explicit SS bound on precision. If many CSs are possible, we obtain the tightest SS bound for $\Delta\varphi_N$ by choosing the 'worst' decomposition yielding minimal $F_{\rm cl}[p_\varphi]$, as shown below. On the other hand, HS is possible only when the above conditions are not satisfied. This happens, for example, in the decoherence-free case where Λ_φ are unitary channels, which are extremal points of the SQC and the only admissible p_φ in equation (4) is the irregular Dirac delta distribution being zero on all channels except Λ_φ.

The QFI at a given φ_0 depends only on the output state and its first derivative at φ_0. This implies that any family of channels $\tilde{\Lambda}_\varphi$,

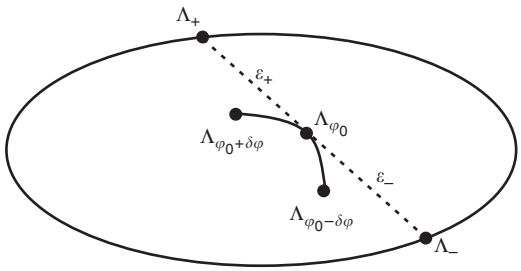

Figure 3 | Local classical stimulation. Schematic representation of a local classical stimulation (CS) of a channel Λ_φ at φ_0 that lies inside the convex set of quantum channels (solid oval). The optimal CS has to be valid only in the neighbourhood of Λ_{φ_0} along the curve $\{\Lambda_\varphi\}_{\varphi_0\pm\delta\varphi}$ (solid arched line) and corresponds to a binary mixture of channels $\Lambda_\pm$, which rest on the tangent (dashed) line at the two outermost points. Then, the precision of estimation can be lower bounded just using the distances $\varepsilon_\pm$.

which 'locally coincides' with the original one, that is,

$$\tilde{\Lambda}_{\varphi_0}[\rho] = \Lambda_{\varphi_0}[\rho],\qquad \partial_\varphi \tilde{\Lambda}_\varphi[\rho]\big|_{\varphi_0} = \partial_\varphi \Lambda_\varphi[\rho]\big|_{\varphi_0}, \tag{8}$$

achieves the same maximum QFI in equation (3). It is therefore enough to consider the 'local classical simulations', that is, any mixtures reproducing the channel and its first derivative at given φ_0. As proven in Supplementary Methods, the CS with the smallest $F_{\rm cl}$ can be constructed using two channels, $\{\Lambda_+,\Lambda_-\}$, which lie on the tangent line to the 'channel trajectory' at the two outermost points situated on the boundary of the set of channels (Fig. 3). The local CS around φ_0 reads explicitly

$$\tilde{\Lambda}_\varphi[\rho] = p_\varphi^+\Lambda_+[\rho] + p_\varphi^-\Lambda_-[\rho], \tag{9}$$

with

$$\Lambda_\pm[\rho] = \Lambda_{\varphi_0}[\rho] \pm \varepsilon_\pm\,\partial_\varphi\Lambda_\varphi[\rho]\big|_{\varphi_0},\quad p_\varphi^\pm = \frac{\varepsilon_\mp \pm (\varphi-\varphi_0)}{\varepsilon_+ + \varepsilon_-}.$$

Making use of equation (7) applied to the binary probability distribution $p_\varphi^\pm$, we obtain

$$\Delta\varphi_N \geq \sqrt{\frac{\varepsilon_+\varepsilon_-}{N}}. \tag{10}$$

To calculate the above bound it suffices to find the 'distances' $\varepsilon_\pm$ of the channel from the boundary measured along the tangent line. For extremal channels, $\varepsilon_\pm = 0$ and the bound is not useful. For non-extremal channels, the above construction will yield a finite $F_{\rm cl}$ provided that $\varepsilon_\pm > 0$, that is, Λ_{φ_0} can be decomposed into a mixture of channels lying on the tangent. Channels that have this additional property will be called 'φ-non-extremal'. They obey the standard precision scaling, and include all full-rank channels (that is, channels lying in the interior of the SQC)[41,42]. An explicit method for calculating $\varepsilon_\pm$ and hence the bound for a general quantum channel is described in the Methods.

Channel extension. Even though the CS method is very general, there are interesting examples of 'φ-extremal' decoherence models for which CS does not apply. In this case, one can resort to the more powerful but less intuitive CE method.

The action of the quantum channel Λ_φ can be described via its Kraus representation[47]:

$$\Lambda_\varphi[\rho] = \sum_i K_i(\varphi)\rho\ K_i^\dagger(\varphi), \tag{11}$$

with Kraus operators satisfying $\Sigma_i K_i(\varphi)^\dagger K_i(\varphi) = \mathbb{1}$. Although this representation is not unique, different sets of linearly independent Kraus operators are related by unitary transformations

$$\tilde{K}_i(\varphi) = \sum_j u_{ij}(\varphi) K_j(\varphi), \tag{12}$$

where $u(\varphi)$ is a unitary matrix possibly depending on φ.

An equivalent definition of the QFI has been proposed[40,42]

$$F_Q\left[\Lambda_\varphi[\rho]\right] = \min_{|\Psi_\varphi\rangle}\ F_Q\left(|\Psi_\varphi\rangle\right), \tag{13}$$

where the minimization is performed over all φ differentiable purifications of the output state

$$\Lambda_\varphi[\rho] = \mathrm{Tr}_E\left\{|\Psi_\varphi\rangle\langle\Psi_\varphi|\right\}. \tag{14}$$

For pure input state, different purifications correspond to different equivalent Kraus representations of the channel, as in equation (12). For many quantum metrological models[40], one can make an educated guess of a purification and derive excellent input-independent analytical bounds providing the correct asymptotic scaling of precision. Nevertheless, the method may be cumbersome especially when the channel description involves many Kraus operators.

A simpler bound can be derived by exploiting the intuitive observation that allowing the channel to act in a trivial way on an extended space, can only improve the precision of estimation, that is,

$$\max_\rho\ F_Q\left[\Lambda_\varphi[\rho]\right] \le \max_{\rho_{\mathrm{ext}}}\ F_Q\left[\Lambda_\varphi \otimes \mathbb{I}[\rho_{\mathrm{ext}}]\right]. \tag{15}$$

This leads to an upper bound on $\mathcal{F}_N$, which goes around the input state optimization, yielding[42]:

$$\mathcal{F}_N \le 4\min_{\tilde{K}}\left\{N\left\|\alpha_{\tilde{K}}\right\| + N(N-1)\left\|\beta_{\tilde{K}}\right\|^2\right\} \tag{16}$$

where $||\cdot||$ denotes the operator norm, the minimization is performed over all equivalent Kraus representations of Λ_φ, and

$$\alpha_{\tilde{K}} = \sum_i \dot{\tilde{K}}_i^\dagger(\varphi)\dot{\tilde{K}}_i(\varphi),\ \beta_{\tilde{K}} = \mathrm{i}\sum_i \dot{\tilde{K}}_i^\dagger(\varphi)\tilde{K}_i(\varphi), \tag{17}$$

where $\dot{\tilde{K}}_i(\varphi) = \partial_\varphi \tilde{K}_i(\varphi)$. For any given $\varphi = \varphi_0$, equation (16) involves only $\tilde{K}_i$ and its first derivatives at φ_0. Moreover, the bound is insensitive to changing the Kraus representations with a φ-independent u. Therefore, it is enough to parameterize equivalent Kraus representations in equation (12) with a hermitian matrix h, which is generator of $u(\varphi) = \exp[-\mathrm{i}h(\varphi - \varphi_0)]$. This reduces the optimization problem equation (16) to a minimization over h.

As the SS of precision holds when $\mathcal{F}_N$ scales linearly with N, the bound equation (16) implies that a sufficient condition for SS is to find h for which $\beta_{\tilde{K}} = 0$, or equivalently[42]:

$$\sum_{i,j} h_{ij} K_i^\dagger K_j = \mathrm{i}\sum_q \dot{K}_q^\dagger K_q. \tag{18}$$

Here we go a step further and show that in this case we can obtain a quantitative SS bound

$$\mathcal{F}_N \le 4N \min_h \left\|\alpha_{\tilde{K}}\right\|, \tag{19}$$

where the minimization runs over h satisfying equation (18), and can be formulated as a semi-definite program, as described in the Methods section.

Moreover, it turns out that the bound resulting from finding the global minimum in equation (19) is at least as tight as the one derived using the CS method based on equation (7) (see Supplementary Methods) proving superiority of the CE over the CS method.

Examples. All examples of channels presented below are of the form $\Lambda_\varphi[\rho] = \Lambda[U_\varphi \rho U_\varphi^\dagger]$, that is, a concatenation of a unitary rotation encoding the estimated parameter φ and an φ-independent decoherence process. Consequently, $K_i(\varphi) = K_i U_\varphi$, where $K_i(\varphi)$, K_i are the Kraus operators of Λ_φ and Λ, respectively. The most relevant models in quantum-enhanced metrology belong to this class, but the methods presented may be applied to more general models as well.

In what follows, we adopt the standard notation where $\mathbb{1}$ is the 2×2 identity matrix and $\{\sigma_i\}_{i=1}^3$ are the Pauli operators. We focus on two-level probe systems (qubits) sensing a phase shift modelled using a unitary $U(\varphi) = \exp[(\mathrm{i}\sigma_3\varphi)/2]$—rotation of the Bloch ball around the z axis. In the case of atomic clocks' frequency calibration $\varphi = \delta\omega \cdot t$ with $\delta\omega$ being the detuning between the frequency of the atomic transition and the frequency of driving field, while t is the time of evolution. Even though in practice the parameter to be estimated is $\delta\omega$, we will consider that to be φ, to have a unified notation for atomic and optical models. In the case of a two-mode optical interferometer, $U(\varphi)$ is the operator acting on a single photon state, accounting for the accumulated relative phase shift φ between the two arms of the interferometer.

We apply the methods to four decoherence processes encountered in quantum-enhanced metrology: two-level atom depolarization, dephasing, spontaneous emission and the photon loss inside the interferometer. These examples will provide us with the full picture of the applicability of the methods discussed in the paper, as their cover all distinct cases from the point of view of the geometry of SQC.

Depolarization. Two-level atom depolarization describes an isotropic loss of coherence and may be visualized by a uniform Bloch ball shrinking (Fig. 4a) where $0 \le \eta < 1$ is the final Bloch ball radius. Its description involves four Kraus operators

$$K_0 = \sqrt{\frac{1+3\eta}{4}}\,\mathbb{1},\quad \left\{K_i = \sqrt{\frac{1-\eta}{4}}\,\sigma_i\right\}_{i=1\ldots3} \tag{20}$$

which makes it an example of a channel lying in the interior of the SQC. Using CS method, we infer the SS of precision and calculate the 'distances' from the boundary of the SQC $\varepsilon_\pm = \sqrt{(1-\eta)(1+3\eta)}/(2\eta)$ (see Methods) resulting in the bound presented in Table 1. Applying

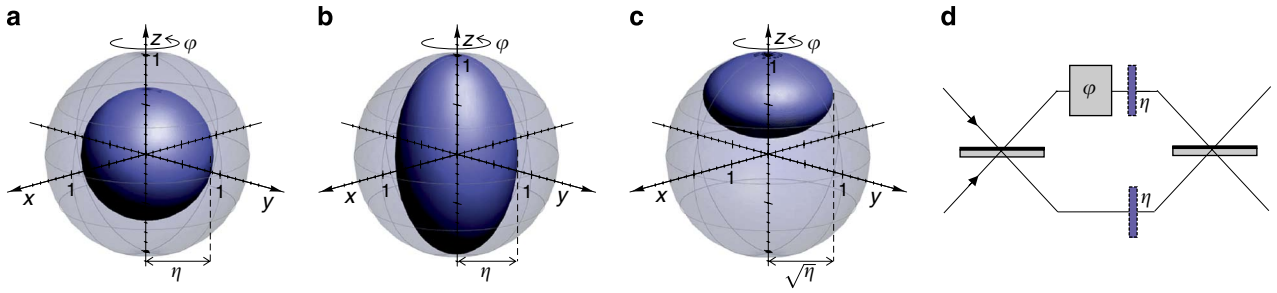

Figure 4 | Graphical representation of decoherence models. Two-level atom decoherence processes are illustrated with a corresponding shrinking of the Bloch ball (blue) for the cases of: (**a**) depolarization, (**b**) dephasing and (**c**) spontaneous emission. The estimated parameter φ represents the angle of rotation about the *z* axis, whereas η specifies the strength of decoherence and effectively the size of shrinkage in the *x*–*y* plane. In the example (**d**) of the lossy interferometer, φ corresponds to the additional phase acquired by photons travelling in the upper arm and η stands for the power transmission coefficient in each of the arms.

Table 1 | Precision bounds of the most relevant models in quantum-enhanced metrology.

Channel considered	Classical simulation	Channel extension
Depolarisation	$\sqrt{(1-\eta)(1+3\eta)/4\eta^2}$	$\sqrt{(1-\eta)(1+2\eta)/2\eta^2}$
Dephasing	$\sqrt{1-\eta^2/\eta}$	$\sqrt{1-\eta^2/\eta}$
Spontaneous emission	NA	$(1/2)\sqrt{1-\eta/\eta}$
Lossy interferometer	NA	$\sqrt{1-\eta/\eta}$

NA, not available.
The bounds are derived using the two methods discussed in the paper. All the bounds are of the form $\Delta\varphi_N \geq (\text{const}/\sqrt{N})$, where constant factors are given in the table. Classical simulation method does not provide bounds for spontaneous emission and lossy interferometer, as these channels are φ-extremal. For the dephasing model, it surprisingly yields an equally tight bound as the more powerful channel extension method.

the CE method, it is possible to further improve the bound and the analytical result of the semi-definite optimization is also shown in Table 1. The only non-zero elements of the corresponding optimal h are $h_{03}=h_{30}=\sqrt{(1-\eta)(1+3\eta)}/c$ and $h_{12}=-h_{21}=-\mathrm{i}(1+\eta)/c$ where $c=2(1-\eta)(1+2\eta)$. To our best knowledge, the bound has not been derived before.

Dephasing. Dephasing is a decoherence model of two-level atoms subject to fluctuating external magnetic/laser fields. In graphical representation, it corresponds to shrinking of the Bloch ball in *x*, *y* directions with *z* direction intact (Fig. 4b). The canonical Kraus operators read[47]

$$K_0=\sqrt{\frac{1+\eta}{2}}\,\mathbb{1},\quad K_1=\sqrt{\frac{1-\eta}{2}}\,\sigma_3, \tag{21}$$

where $0\leq\eta<1$ is the dephasing parameter. As it involves only two Kraus operators, it is not a full-rank channel and lies on the boundary of the SQC. It is, however, a non-extremal and more importantly φ-non-extremal channel allowing for the CS construction with $\varepsilon_{\pm}=\sqrt{1-\eta^2}/\eta$ (see Methods), yielding the bound given in Table 1.

Most importantly, the above bound, is exactly the same as the one derived by Escher *et al.*[40] or by the CE method, where the minimum in equation (19) corresponds to $h=\sigma_1/\left(2\sqrt{1-\eta^2}\right)$. This proves that despite its simplicity the CS method may sometimes lead to bounds that are equally tight as the ones derived with much more advanced methods even for channels lying on the boundary of the SQC.

Spontaneous emission. The well-known two-level atom spontaneous emission model is described by the Kraus operators

$$K_0=\begin{pmatrix}1&0\\0&\sqrt{\eta}\end{pmatrix},\quad K_1=\begin{pmatrix}0&\sqrt{1-\eta}\\0&0\end{pmatrix} \tag{22}$$

with $0\leq\eta<1$. Interestingly, for all η this channel is extremal[48], which means that the CS is not applicable. Nevertheless, the CE method of equation (19) can be easily employed.

Substituting $K_i(\varphi)$ into equation (18), we find that the generator h is fixed to $h=\frac{1}{2(1-\eta)}(\sigma_z-\eta\mathbb{1})$. Consequently, there is no need for minimization over h and from equation (19) we automatically obtain an SS bound listed in Table 1, which to our knowledge has not been reported in the literature before.

Lossy interferometer. To model 'loss' in an optical interferometer, a third orthogonal state at the output,—vacuum—resulting from a loss of a photon, needs to be introduced. The decoherence channel on a single probe (single photon) is a map from a two- to a three-dimensional system:

$$K_0=\begin{pmatrix}0&0\\0&0\\0&\sqrt{1-\eta}\end{pmatrix},\quad K_1=\begin{pmatrix}0&0\\0&0\\\sqrt{1-\eta}&0\end{pmatrix},\quad K_2=\begin{pmatrix}\sqrt{\eta}&0\\0&\sqrt{\eta}\\0&0\end{pmatrix}, \tag{23}$$

where η is the power transmission coefficient for the light travelling through each of the two arms. Although the corresponding channel Λ_φ is non-extremal, it is unfortunately φ-extremal and CS cannot be used. Still, CE method can be easily applied. The optimal bound (see Table 1) corresponds to h with non-zero elements $h_{00}=-h_{11}=\frac{1}{2(1-\eta)}$. This bound is asymptotically equally tight to the best bounds known in the literature[38–40], proving again that CE method despite its simplicity is able to provide powerful results in a straightforward manner.

In optical interferometric applications, it is common to use states of light with an unbounded number of photons, such as coherent or squeezed states[49–53]. At a first glance, it is not obvious that the model considered in the paper covers these situations. Formally speaking, the bound we have derived applies to input states with a total number of photons fixed to *N*. Notice, however, that in every

optical experiment what is measured in the end are photon numbers. If all phase reference beams are taken into account, we can regard quantum states of light as incoherent mixtures of states occupying different total photon number sectors[53,54]. From the point of view of metrology, the QFI is then bounded from above by the weighted sum of QFIs for each of these sectors[30]. Within each sector we can easily apply our bound and, as the bound is linear in N, the effective bound will simply correspond to replacing N with $\bar{N}$—the mean number of photons in all relevant beams used in the experiment—and as such can be automatically applied to experiments involving coherent and squeezed light.

To demonstrate the practical relevance of the bound, it is instructive to compare its predictions with the actual quantum enhancement observed recently in the GEO600 gravitational wave detector[17]. Although a detailed theoretical analysis of the set-up from the perspective of the derived bounds is still underway, by reducing the essential features of the set-up to a simple Mach–Zehnder interferometer, we can already give a preliminary estimate on how far is the actual experiment from the optimal performance. For the reported overall optical transmission $\eta=0.62$, the theoretically predicted maximal quantum enhancement amounts to a $\sqrt{1-\eta}=0.62$ factor reduction in estimation uncertainty compared with the classical $1/\sqrt{\eta\bar{N}}$ limit. The reported experimentally observed reduction was a factor of 0.67, which is an indication that the experiment operates close to the fundamental quantum limit and any significant improvement is possible only if the optical loss is further reduced.

Discussion

Assessing the impact of decoherence on the maximum possible quantum enhancement is a crucial element in developing quantum techniques for metrological applications. The tools developed here allow for a direct calculation of bounds on the precision enhancement for arbitrary parameter estimation model where the decoherence process acts independently on each of the probes and may be represented with a finite number of Kraus operators. The CE method is more powerful and for the most relevant metrological models yields in the asymptotic limit of large number of probes the tightest bounds known in the literature. Yet the CS method, which may fail to provide equally tight bounds, provides an intuitive geometric insight into the absence of asymptotic HS in the presence of decoherence. From the derived bounds, it is clear that if the HS was to be preserved for large number of probes N the level of decoherence would have to decrease with increasing N roughly as $(1-\eta)\approx 1/N$. This gives an estimate on the regime in which the quantum enhancement is quadratic as compared with the regime of constant factor improvement. This is clearly seen in Fig. 2 where this transition appears around $N\approx 1/(1-\eta)=20$ for $\eta=0.95$. As in most metrology applications N is larger by several order of magnitude, we expect that the SS scaling provides a reliable bound for the optimal estimation precision.

An important question that was not addressed here is the saturability of the bounds. The CS method does not provide tight bounds in general. As for the CE method, we are not able to prove that the bounds we have derived are saturable in the asymptotic limit. We should stress however, that these are lower bounds on estimation uncertainties and an upper bound can always be found by choosing a particular estimation method. Therefore, if a certain strategy performs close to the derived bound, we can certify that it is not far from reaching the fundamental quantum limit, as illustrated by the results of the GEO600 experiment.

Even though the minimization over purification method[40] yields in principle a tight bound, in practice there is no effective algorithm to find a global minimum, and the only way to convince oneself that one has achieved the global minimum is again to show that the theoretical lower bound on estimation uncertainty coincides with the performance of a particular estimation strategy.

The methods discussed were focused on deriving useful bounds in the asymptotic regime of a large number of probes. Still, the bounds are valid (though weaker) for any value of N. We leave it for a future work to improve the bounds for finite N, which seems to be possible by using the CE method and relaxing the $\beta_{\tilde{K}}=0$ constraint.

Methods

Proof of the CS bound. To simplify the reasoning, let us focus on the CSs that are constructed using discrete sets of quantum channels, $\{\Lambda_i\}$. Then, the considered channel's action of equation (4) can be rewritten as a φ-independent map acting on a larger input space[41]

$$\Lambda_\varphi[\rho]=\sum_i p_{\varphi,i}\Lambda_i[\rho]=\Phi\left[\rho\otimes\sigma_\varphi\right], \tag{24}$$

where $\sigma_\varphi=\Sigma_i p_{\varphi,i}\,|e_i\rangle\langle e_i|$ represents a diagonal state in some basis, in which Φ is defined via $\Phi[\rho]=\Sigma_i(\Lambda_i\otimes E_i)[\rho]$ with $E_i[\sigma]=\langle e_i|\sigma|e_i\rangle$. To prove equation (7), we write the QFI for the N parallel use of the channel and bound it from above, that is

$$\begin{aligned} &F_Q\left[\Lambda_\varphi^{\otimes N}[\rho]\right]=F_Q\left[\Phi^{\otimes N}\left[\rho\otimes\sigma_\varphi^{\otimes N}\right]\right]\\ &\le F_Q\left[\rho\otimes\sigma_\varphi^{\otimes N}\right]=F_Q\left[\sigma_\varphi^{\otimes N}\right]=N\,F_Q\left[\sigma_\varphi\right]=N\,F_{\mathrm{cl}}\left[p_\varphi\right], \end{aligned} \tag{25}$$

exploiting the monotonicity of the QFI under any parameter-independent quantum map[55], here $\Phi^{\otimes N}$.

Calculation of the CS bound. The geometry of the space of channels and more specifically the φ-extremality are best viewed by using the Choi–Jamiołkowski isomorphism[56,57]. Given a quantum channel $\Lambda:\mathcal{L}(\mathcal{H}_{\mathrm{in}})\mapsto\mathcal{L}(\mathcal{H}_{\mathrm{out}})$ acting from the space of density matrices on $\mathcal{H}_{\mathrm{in}}$ to density matrices on $\mathcal{H}_{\mathrm{out}}$, one defines $P_\Lambda=\Lambda\otimes\mathbb{I}[|\Psi\rangle\langle\Psi|]$, where $|\Psi\rangle=\sum_{i=1}^{d_{\mathrm{in}}}|i\rangle\otimes|i\rangle$ is a maximally entangled state in $\mathcal{H}_{\mathrm{in}}\otimes\mathcal{H}_{\mathrm{in}}$. Λ is a physical channel (that is, trace preserving, completely positive map) if P_Λ is a positive semi-definite operator, satisfying $\mathrm{Tr}_{\mathcal{H}_{\mathrm{out}}}\{P_\Lambda\}=\mathbb{1}$. If $\{K_i\}_i$ are the Kraus operators of the Λ channel, we can write explicitly $P_\Lambda=\Sigma_i\,|K_i\rangle\!\rangle\langle\!\langle K_i|$, where $|K_i\rangle\!\rangle=K_i\otimes\mathbb{1}\,|\Psi\rangle$.

We can now say that the channel Λ_φ is φ-non-extremal, if it is possible to find a non-zero ε, for which $P_{\Lambda_\varphi}\pm\varepsilon\partial_\varphi P_{\Lambda_\varphi}\ge 0$. See Supplementary Methods for an alternative formulation of the φ-non-extremality condition and its relation to the well-known non-extremality condition due to Choi[57]. In practice, if we want to make most out of the bound in equation (10), we need to find the maximum values of $\varepsilon_\pm$, for which $P_{\Lambda_\varphi}\pm\varepsilon_\pm\partial_\varphi P_{\Lambda_\varphi}$ are still positive semi-definite operators. This is a simple eigenvalue problem and therefore the bound can be obtained immediately.

Taking the dephasing model as an example, the Choi–Jamiołkowski isomorphism of the corresponding Λ_φ channel $P_{\Lambda_\varphi}=\Sigma_{i=1}^2|K_iU_\varphi\rangle\!\rangle\langle\!\langle K_iU_\varphi|$ has a simple form:

$$P_{\Lambda_\varphi}=\begin{pmatrix} 1 & 0 & 0 & \eta e^{i\varphi}\\ 0 & 0 & 0 & 0\\ 0 & 0 & 0 & 0\\ \eta e^{-i\varphi} & 0 & 0 & 1\end{pmatrix}. \tag{26}$$

It is easy to check that $P_{\Lambda_\varphi}+\varepsilon\partial_\varphi P_{\Lambda_\varphi}\ge 0$ provided $|\varepsilon|\le\sqrt{1-\eta^2}/\eta$, hence using equation (10) we arrive at the bound given in Table 1.

CE method as a semi-definite program. Here we show that the minimization problem in equation (19) can be formulated as a simple semi-definite program. Let the channel Λ_φ be a map from a d_1- to a d_2-dimensional Hilbert spaces with Kraus representation involving k linear independent Kraus operators ($d_2\times d_1$ matrices). Consider the following block matrix:

$$A=\begin{pmatrix} \sqrt{t}\mathbb{1}_{d_1} & \dot{\tilde{K}}_0^\dagger & \dot{\tilde{K}}_1^\dagger & \dots & \dot{\tilde{K}}_{k-1}^\dagger\\ \dot{\tilde{K}}_0 & \sqrt{t}\mathbb{1}_{d_2} & 0 & \dots & 0\\ \dot{\tilde{K}}_1 & 0 & \sqrt{t}\mathbb{1}_{d_2} & \dots & 0\\ \vdots & \vdots & \vdots & \ddots & \vdots\\ \dot{\tilde{K}}_{k-1} & 0 & 0 & \dots & \sqrt{t}\mathbb{1}_{d_2}\end{pmatrix}, \tag{27}$$

where $\mathbb{1}$ is a $d\times d$ identity matrix. Positive semi-definiteness of the matrix A is equivalent to the condition

$$\alpha_{\tilde{K}} = \sum_i \dot{\tilde{K}}_i^\dagger \dot{\tilde{K}}_i \le t\mathbb{1}_{d_1}. \tag{28}$$

Minimizing the operator norm $\|\alpha_{\tilde{K}}\|$ is thus equivalent to minimizing t subject to $A\ge 0$. Taking into account equation (18), the problem takes the form:

$$\min_h t, \quad \text{subject to}: A\ge 0, \sum_{ij} h_{ij} K_i^\dagger K_j = \mathrm{i}\sum_q \dot{K}_q^\dagger K_q. \tag{29}$$

Since $\dot{\tilde{K}}_i = \dot{K}_i - \mathrm{i}\Sigma_j h_{ij} K_j$ the matrix A is linear in h and the problem is thus a semi-definite program with the resulting minimal t being the minimal operator norm $\|\alpha_{\tilde{K}}\|$. For the purpose of this paper, we have implemented the program using the CVX package for Matlab[58].

References

1. Giovannetti, V., Lloyd, S. & Maccone, L. Advances in quantum metrology. *Nat. Photon.* **5,** 222–229 (2011).
2. Maccone, L. & Giovannetti, V. Quantum metrology: beauty and the noisy beast. *Nat. Phys.* **7,** 376–377 (2011).
3. Paris, M. G. A. Quantum estimation for quantum technology. *Int. J. Quant. Inf.* **7,** 125–137 (2009).
4. Banaszek, K., Demkowicz-Dobrzanski, R. & Walmsley, I. A. Quantum states made to measure. *Nat. Photon.* **3,** 673–676 (2009).
5. Dirac, P. A. M. *The Principles of Quantum Mechanics* (Oxford University Press, 1958).
6. Kahn, J. & Guţă, M. Local asymptotic normality for finite dimensional quantum systems. *Commun. Math. Phys.* **289,** 597–652 (2009).
7. Giovannetti, V., Lloyd, S. & Maccone, L. Quantum-enhanced measurements: beating the standard quantum limit. *Science* **306,** 1330–1336 (2004).
8. Giovannetti, V., Lloyd, S. & Maccone, L. Quantum metrology. *Phys. Rev. Lett.* **96,** 010401 (2006).
9. Braunstein, S. L. & Caves, C. M. Statistical distance and the geometry of quantum states. *Phys. Rev. Lett.* **72,** 3439–3443 (1994).
10. Berry, D. W. & Wiseman, H. M. Optimal states and almost optimal adaptive measurements for quantum interferometry. *Phys. Rev. Lett.* **85,** 5098–5101 (2000).
11. Zwierz, M., Prez-Delgado, C. A. & Kok, P. General optimality of the heisenberg limit for quantum metrology. *Phys. Rev. Lett.* **105,** 180402 (2010).
12. Mitchell, M. W., Lundeen, J. S. & Steinberg, A. M. Super-resolving phase measurements with a multi-photon entangled state. *Nature* **429,** 161–164 (2004).
13. Eisenberg, H. S., Hodelin, J. F., Khoury, G. & Bouwmeester, D. Multiphoton path entanglement by nonlocal bunching. *Phys. Rev. Lett.* **94,** 090502 (2005).
14. Nagata, T., Okamoto, R., O'Brien, J. L., Sasaki, K. & Takeuchi, S. Beating the standard quantum limit with four entangled photons. *Science* **316,** 726–729 (2007).
15. Resch, K. J. *et al.* Time-reversal and super-resolving phase measurements. *Phys. Rev. Lett.* **98,** 223601 (2007).
16. Higgins, B. L. *et al.* Demonstrating heisenberg-limited unambiguous phase estimation without adaptive measurements. *New J. Phys.* **11,** 073023 (2009).
17. LIGO Collaboration.. A gravitational wave observatory operating beyond the quantum shot-noise limit. *Nat. Phys.* **7,** 962–965 (2011).
18. Goda, K. *et al.* A quantum-enhanced prototype gravitational-wave detector. *Nat. Phys.* **4,** 472–476 (2008).
19. Wineland, D. J., Itano, W. M., Bollinger, J. J. & Moore, F. L. Spin squeezing and reduced quantum noise in spectroscopy. *Phys. Rev. A* **46,** R6797–R6800 (1992).
20. Huelga, S. F. *et al.* Improvement of frequency standards with quantum entanglement. *Phys. Rev. Lett.* **79,** 3865–3868 (1997).
21. Meyer, V. *et al.* Experimental demonstration of entanglement-enhanced rotation angle estimation using trapped ions. *Phys. Rev. Lett.* **86,** 5870–5873 (2001).
22. Leibfried, D. *et al.* Toward heisenberg-limited spectroscopy with multiparticle entangled states. *Science* **304,** 1476–1478 (2004).
23. Wasilewski, W. *et al.* Quantum noise limited and entanglement-assisted magnetometry. *Phys. Rev. Lett.* **104,** 133601 (2010).
24. Koschorreck, M., Napolitano, M., Dubost, B. & Mitchell, M. W. Sub-projection-noise sensitivity in broadband atomic magnetometry. *Phys. Rev. Lett.* **104,** 093602 (2010).
25. Higgins, B. L., Berry, D. W., Bartlett, S. D., Wiseman, H. M. & Pryde, G. J. Entanglement-free heisenberg-limited phase estimation. *Nature* **450,** 393–396 (2007).
26. Demkowicz-Dobrzanski, R. Multi-pass classical versus quantum strategies in lossy phase estimation. *Laser Phys.* **20,** 1197–1202 (2010).
27. Boixo, S., Flammia, S. T., Caves, S. T. & Geremia, J. M. Generalized limits for single-parameter quantum estimation. *Phys. Rev. Lett* **98,** 090401 (2007).
28. Napolitano, M. *et al.* Interaction-based quantum metrology showing scaling beyond the Heisenberg limit. *Nature* **471,** 486–489 (2011).
29. Dorner, U. *et al.* Optimal quantum phase estimation. *Phys. Rev. Lett.* **102,** 040403 (2009).
30. Demkowicz-Dobrzański, R. *et al.* Quantum phase estimation with lossy interferometers. *Phys. Rev. A* **80,** 013825 (2009).
31. Shaji, A. & Caves, C. M. Qubit metrology and decoherence. *Phys. Rev. A* **76,** 032111 (2007).
32. Andrè, A., Sorensen, A. S. & Lukin, M. D. Stability of atomic clocks based on entangled atoms. *Phys. Rev. Lett.* **92,** 230801 (2004).
33. Meiser, D. & Holland, M. J. Robustness of heisenberg-limited interferometry with balanced fock states. *New J. Phys.* **11,** 033002 (2009).
34. Zhengfeng, J., Guoming, W., Runyao, D., Yuan, F. & Mingsheng, Y. Parameter estimation of quantum channels. *IEEE Trans. Inf. Theory* **54,** 5172–5185 (2008).
35. Datta, A. *et al.* Quantum metrology with imperfect states and detectors. *Phys. Rev. A* **83,** 063836 (2011).
36. Kacprowicz, M., Demkowicz-Dobrzanski, R., Wasilewski, W., Banaszek, K. & Walmsley, I. A. Experimental quantum enhanced phase-estimation in the presence of loss. *Nat. Photon.* **4,** 357–360 (2010).
37. Thomas-Peter, N. *et al.* Real-world quantum sensors: evaluating resources for precision measurement. *Phys. Rev. Lett.* **107,** 113603 (2011).
38. Kołodyński, J. & Demkowicz-Dobrzański, R. Phase estimation without *a priori* phase knowledge in the presence of loss. *Phys, Rev. A* **82,** 053804 (2010).
39. Knysh, S., Smelyanskiy, V. N. & Durkin, G. A. Scaling laws for precision in quantum interferometry and the bifurcation landscape of the optimal state. *Phys. Rev. A* **83,** 021804(R) (2011).
40. Escher, B. M., de Matos Filho, R. L. & Davidovich, L. General framework for estimating the ultimate precision limit in noisy quantum-enhanced metrology. *Nat. Phys.* **7,** 406–411 (2011).
41. Matsumoto, K. On metric of quantum channel spaces. Preprint at arxiv: 1006.0300 (2010).
42. Fujiwara, A. & Imai, H. A fibre bundle over manifolds of quantum channels and its application to quantum statistics. *J. Phys. A: Math. Theor.* **41,** 255304 (2008).
43. Bollinger, J. J., Itano, W. M., Wineland, D. J. & Heinzen, D. J. Optimal frequency measurements with maximally correlated states. *Phys. Rev. A* **54,** R4649–R4652 (1996).
44. Dowling, J. P. Correlated input-port, matter-wave interferometer: quantum-noise limits to the atom-laser gyroscope. *Phys. Rev. A* **57,** 4736–4746 (1998).
45. Bengtsson, I. & Zyczkowski, K. *Geometry of Quantum States: An Introduction to Quantum Entanglement* (Cambridge Univeristy Press, 2006).
46. Kay, S. M. *Fundamentals of Statistical Signal Processing: Estimation Theory*, Prentice Hall, 1993.
47. Nielsen, M. A. & Chuang, I. L. *Quantum Computing and Quantum Information* (Cambridge University Press, 2000).
48. Ruskai, M. B., Szarek, S. & Werner, E. An analysis of completely-positive trace-preserving maps on 2×2 matrices. *Lin. Alg. Appl.* **347,** 159–187 (2002).
49. Caves, C. M. Quantum-mechanical noise in an interferometer. *Phys. Rev. D.* **23,** 1693–1708 (1981).
50. Pezze, L. & Smerzi, A. Mach-Zehnder interferometry at the Heisenberg limit with coherent and squeezed-vacuum light. *Phys. Rev. Lett.* **100,** 073601 (2008).
51. Genomi, M. G., Olivares, S. & Paris, M. G. A. Optical phase estimation in the presence of phase-diffusion. *Phys. Rev. Lett.* **106,** 153603 (2011).
52. Pinel, O. *et al.* Ultimate sensitivity of precision measurements with intense Gaussian quantum light: a multimodal approach. *Phys. Rev. A* **85,** 010101(R) (2012).
53. Jarzyna, M. & Demkowicz-Dobrzanski, R. Quantum interferometry with and without an external phase reference. *Phys. Rev. A* **85,** 011801(R) (2012).
54. Molmer, K. Optical coherence: a convenient fiction. *Phys. Rev. A* **55,** 3195 (1996).
55. Fujiwara, A. Quantum channel identification problem. *Phys. Rev. A* **63,** 042304 (2001).
56. Jamiolkowski, A. Linear transformations which preserve trace and positive semidefiniteness of operators. *Rep. Math. Phys* **3,** 275–278 (1972).
57. Choi, M.- D. Completely positive linear maps on complex matrices. *Lin. Algebr. Appl.* **10,** 285–290 (1975).
58. Grant, M. & Boyd, S. CVX: Matlab software for disciplined convex programming, http://cvxr.com/cvx/ (2011).

Acknowledgements

We thank Konrad Banaszek for many inspiring discussions and constant support. R.D.-D. and J.K. were supported by the European Commission under the IP project Q-ESSENCE, ERA-NET CHIST-ERA project QUASAR and the Foundation for Polish Science under the TEAM programme. M.G. was supported by the EPSRC Fellowship EP/E052290/1.

Author contributions

M.G. conceived the CS method. J.K. developed the CE method and utilized both approaches to obtain the exemplary analytic results. R.D.-D. proved the optimality of local tangent CS, the relation between the methods and formulated the semi-definite programming approach to CE. All authors contributed extensively to the manuscript with the leading input from R.D.-D.

Additional information

Supplementary Information accompanies this paper at http://www.nature.com/naturecommunications

Competing financial interests: The authors declare no competing financial interests.

Reprints and permission information is available online at http://npg.nature.com/reprintsandpermissions/

How to cite this article: Demkowicz-Dobrzański, R. *et al.* The elusive Heisenberg limit in quantum-enhanced metrology. *Nat. Commun.* 3:1063 doi: 10.1038/ncomms2067 (2012).

Efficient tools for quantum metrology with uncorrelated noise

Jan Kołodyński and Rafał Demkowicz-Dobrzański

Faculty of Physics, University of Warsaw, 00-681 Warszawa, Poland

E-mail: jankolo@fuw.edu.pl and demko@fuw.edu.pl

Abstract. Quantum metrology offers an enhanced performance in experiments such as gravitational wave-detection, magnetometry or atomic clocks frequency calibration. The enhancement, however, requires a delicate tuning of relevant quantum features such as entanglement or squeezing. For any practical application the inevitable impact of decoherence needs to be taken into account in order to correctly quantify the ultimate attainable gain in precision. We compare the applicability and the effectiveness of various methods of calculating the ultimate precision bounds resulting from the presence of decoherence. This allows us to put a number of seemingly unrelated concepts into a common framework and arrive at an explicit hierarchy of quantum metrological methods in terms of the tightness of the bounds they provide. In particular, we show a way to extend the techniques originally proposed in Demkowicz-Dobrzański R, Kołodyński J and Guţă M 2012 *Nat. Commun.* **3** 1063, so that they can be efficiently applied not only in the asymptotic but also in the finite-number of particles regime. As a result we obtain a simple and direct method yielding bounds that interpolate between the quantum enhanced scaling characteristic for small number of particles and the asymptotic regime, where quantum enhancement amounts to a constant factor improvement. Methods are applied to numerous models including noisy phase and frequency estimation as well as the estimation of the decoherence strength itself.

PACS numbers: 03.67.-a, 03.65.Yz, 03.65.Ud, 03.65.Ta, 42.50.St

1. Introduction

Quantum enhanced metrology has recently enjoyed a great success at experimental level leading to new results in atomic spectroscopy [1–4], magnetometry [5–7] and optical interferometry [8–11] with prominent achievements in gravitational waves sensing [12]. As predicted in the incipient theoretical results of [13–17], a physical parameter unitarily encoded into a quantum system — probe — consisting of N entangled, non-interacting particles (atoms or photons) can be extracted with precision that is limited by the quantum-mechanical uncertainty relations and not the more restrictive central limit theorem of classical statistics. Hence, the uncertainty in reconstructing the encoded parameter, such as e.g. optical phase delay or frequency difference, can in principle be proportional to $1/N$, the so-called *Heisenberg Limit* (HL), rather than $1/\sqrt{N}$, commonly referred to as the *Standard Quantum Limit* (SQL) or the shot (projection) noise. However, this dramatic scaling improvement can be illusive, as both the experimental results and theoretical toy-models have indicated that achieving the ideal HL is a hard task owing to the strong destructive impact of imperfections, which should be always accounted for in realistic scenarios.

An important question that has been considerably addressed by many researchers [18–32] reads: how and to what extent can the noise effects be compensated in quantum metrological setups? In the case of atomic spectroscopy, it has already been indicated in [24, 25] that the effects of uncorrelated noise, independently affecting the atoms within a probe, have a dramatic impact on quantum protocols — most likely restricting the ultimate precision scaling to become SQL-like for high enough N, so that the quantum enhancement is asymptotically limited to a multiplicative *constant factor*. In optical interferometry, photonic loss is the main obstacle to practical implementations of quantum enhanced protocols [27–30] and the asymptotic SQL-like scaling is again inevitable, as proven in [31, 32]. Similarly to the atomic case, the asymptotic improvement constant becomes an essential feature which determines the achievable precision for high N. Following the above exemplary models, methods of quantifying the asymptotic quantum enhancement have been proposed for arbitrary kinds of probes with decoherence present [33–39]. Recently, general procedures have been established that are capable of deriving practical bounds on ultimate achievable precision in realistic quantum metrological setups [38, 39]. In particular, in the case of uncorrelated noise it has been demonstrated that the sole analysis of the evolution of a *single* particle often leads to surprisingly informative bounds on the precision achievable with arbitrarily entangled multi-particle inputs [39] — see Figure 1 for a summary of the single particle (single channel) methods investigated further on in this paper. For completeness, it should be noted that there are some specific metrological models *with* noise, in which asymptotic scaling power enhancement *is* nevertheless possible [22, 23, 40]. Still, applicability of these models is limited, since in any practical implementation the noise types considered will always be accompanied by some generic decoherence processes for which the constant factor bound on the maximal quantum

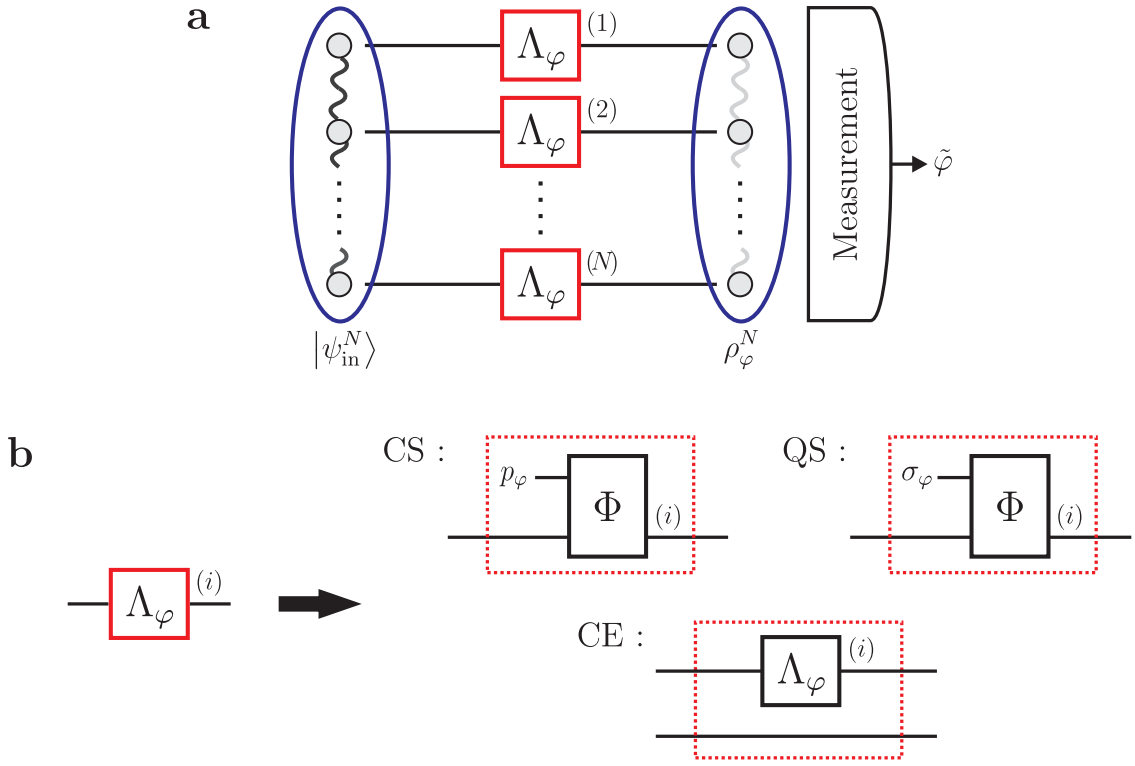

Figure 1. Quantum metrology and the single channel methods
(**a**) General scheme for quantum-enhanced metrology with uncorrelated noise. The N particles within the probe in a quantum state $\psi_{\rm in}^N$ evolve and decohere independently while sensing an unknown parameter φ (e.g. phase). An estimate $\tilde{\varphi}$ of the parameter is inferred from a measurement result on the final state of the probe ρ_φ^N.
(**b**) Precision bounds from single channel analysis. The ultimate precision is bounded by the $1/\sqrt{N}$ scaling (SQL), if for small variations $\delta\varphi$ around φ the channel Λ_φ can be expressed as a parameter-independent map Φ that is also fed a classical, diagonal state p_φ, classical simulation (CS), or a general, quantum state σ_φ, quantum simulation (QS), varying smoothly with φ. Still, for all such channels and more, the tightest bound on precision is obtained by the channel extension (CE) method, in which the map Λ_φ is replaced by its extension $\Lambda_\varphi \otimes \mathcal{I}$.

enhancement will force the asymptotic precision scaling to be SQL-like.

In this paper, we provide new insight into relations between seemingly unrelated methods used for derivations of various quantum metrological bounds and order them with respect to their predictive power. Firstly, focussing on the geometric intuitive method of channel *classical simulation* (CS) introduced in [36, 39], we prove that its applicability is equivalent to the approach proposed in [37]. Moreover, we show that the criterion for classical simulability of a channel can be generalized to a *quantum simulability* (QS) condition [36], which coincides with the channel programmability postulate of [34]. Although the idea of QS allows to prove the asymptotic SQL-like behaviour for a wider range of decoherence models, we demonstrate that the *channel extension* (CE) method of [39] encompasses all CS, [37], QS and [34] approaches providing more stringent bounds on precision. We also comment on the problem of

the tightness of these bounds, as they are guaranteed to be saturable only for channels, for which the estimation task cannot be improved by allowing for an additional ancilla (extension, idler mode) entangled with the input state. Classification of such channels is an open problem of current research in channel estimation [41–44] and akin channel discrimination [45–53] theory. The graphical interpretation of the CS, QS and CE methods is presented in Figure 1**b**.

Most importantly, we go beyond the results of [39] and show that the CE method may be applied not only in the asymptotic regime but also when dealing with finite probes of N particles. Similarly to the asymptotic case, it corresponds then to an optimisation procedure over Kraus representations of a given channel that can be recast into an efficiently solvable semi-definite programming task. We apply our results to phase/frequency estimation with various noise models including: dephasing, depolarization, loss and spontaneous emission; restricting ourselves to the cases of noise commuting with the parameterized unitary part of the evolution. This assumption makes the analysis more transparent, but is not indispensable, since our methods may be effectively employed for any single particle evolution described by a general Lindblad equation [54] reshaped into the corresponding Kraus representation [55]. What is more, as our finite-N CE method applies to models for which its asymptotic version fails, it can be used to upper-bound the asymptotic scaling for channels surpassing the SQL. As an example, in [40], our new method has been already utilized to predict asymptotic super-classical scaling for a channel with a non-commutative noise. Additionally, in order to stress the generality of the methods, in the final section of this paper we show that they can be applied not only to noisy unitary parameter estimation tasks but also to ones in which the decoherence strength itself is estimated. Finally, we should also clarify that noise correlation and memory effects [56, 57] are beyond the scope of this paper and while the non-Markovian effects, provided they affect each of the particles independently, might be analyzed using the tools presented, correlations between the decoherence processes affecting the particles does not fit well into the framework here advocated.

2. Quantum Fisher Information

2.1. Classical Cramér-Rao bound

Let us assume that after measuring a physical system an outcome is obtained that can be represented by a random variable X distributed with some probability distribution $p_\varphi(X)$. If the system is classically described, all its properties can be simultaneously determined, so that X can in principle be multidimensional and contain as much information about the system as allowed by the available resources. The estimation task corresponds then to determining with highest precision the quantity φ based on the observed value of X. As stated by the *Cramér-Rao bound* [58] any unbiased strategy to determine the unknown parameter after repeating the procedure k times, must provide

an estimate $\tilde{\varphi}$ with uncertainty that is lower bounded by

$$\Delta\tilde{\varphi} \geq \frac{1}{\sqrt{k\, F_{\rm cl}[p_\varphi]}}\,, \qquad \text{where} \qquad F_{\rm cl}[p_\varphi] = \int\!dx\, \frac{\dot{p}_\varphi(x)^2}{p_\varphi(x)} \tag{1}$$

is the (*classical*) *Fisher Information* (FI) ‡.

The $1/\sqrt{k}$ dependence in (1) is a consequence of the central limit theorem and the fact that the k procedures are independent. This manifests itself by the additivity property of the FI, i.e. $F_{\rm cl}\big[p_\varphi^k\big] = k\, F_{\rm cl}[p_\varphi]$ for X^k. Equation (1) shows that the FI is a *local* quantity containing information about infinitesimal variations of φ. That is why, FI is designed to be used in the so called *local estimation* approach in which small parameter fluctuations are to be sensed. This small deviations regime may always be reached after many procedure repetitions ($k \to \infty$) and in this limit the Cramér-Rao bound is known to be saturable via e.g. max-likelihood estimation schemes [58].

2.2. Quantum Cramér-Rao bound

In a quantum estimation scenario, the parameter φ is encoded in a quantum state ρ_φ. A general measurement, mathematically represented by the elements of the *positive operator valued measure* (POVMs) M_x that satisfy $M_x \geq 0$, $\int\!dx\, M_x = \mathbb{I}$ § [59, 60], is performed yielding outcome statistics $p_\varphi(X) = \mathrm{Tr}\{\rho_\varphi M_X\}$. Establishing the optimal estimation strategy corresponds then not only to the correct interpretation of the measurement results, but also to a non-trivial optimization over the class of all POVMs to find the measurement scheme maximizing the precision. In this case the *Quantum Cramér-Rao bound* can be derived [61–63], which is independent of the choice of the POVMs and solely determined by the dependence of the output state on the estimated parameter:

$$\Delta\tilde{\varphi} \geq \frac{1}{\sqrt{k\, F_{\rm Q}[\rho_\varphi]}} \qquad \text{with} \qquad F_{\rm Q}[\rho_\varphi] = \mathrm{Tr}\Big\{\rho_\varphi\, L^{\rm S}[\rho_\varphi]^2\Big\} \tag{2}$$

being now the *Quantum Fisher Information* (QFI). The Hermitian operator $L^{\rm S}[\rho_\varphi]$ is the so called *Symmetric Logarithmic Derivative* (SLD), which can be unambiguously defined for any state ρ_φ via the relation $\dot{\rho}_\varphi = \frac{1}{2}\left(\rho_\varphi L^{\rm S}[\rho_\varphi] + L^{\rm S}[\rho_\varphi]\rho_\varphi\right)$. Then, in the eigenbasis of $\rho_\varphi = \sum_i \lambda_i(\varphi)\, |e_i(\varphi)\rangle\langle e_i(\varphi)|$ with $\{|e_i(\varphi)\rangle\}_i$ forming a complete basis ($\forall_i\colon\, 0 \leq \lambda_i \leq 1$)

$$L^{\rm S}[\rho_\varphi] = \sum_{i,j} \frac{2\,\langle e_i(\varphi)|\,\dot{\rho}_\varphi\,|e_j(\varphi)\rangle}{\lambda_i(\varphi) + \lambda_j(\varphi)}\, |e_i(\varphi)\rangle\langle e_j(\varphi)|\,, \tag{3}$$

where the sum is taken over the terms with non-vanishing denominator. QFI is additive on product states and in particular $F_{\rm Q}\big[\rho_\varphi^{\otimes k}\big] = k\, F_{\rm Q}[\rho_\varphi]$. Thus, the $\sqrt{k}$ term in the denominator of (2) may be equivalently interpreted as the number of independent repetitions of an experiment with a state ρ_φ or a single shot experiment with a multi-party state $\rho_\varphi^{\otimes k}$. Crucially, as proven in [63, 64], there always exist a measurement

‡ Throughout the paper, we depict derivatives w.r.t. the estimated parameter with an 'overdot', so that e.g. $\dot{p}_\varphi(x) \equiv \partial_\varphi\, p_\varphi(x)$, $\dot{\rho}_\varphi \equiv \partial_\varphi\, \rho_\varphi$ and $\dot{K}(\varphi) \equiv \partial_\varphi\, K(\varphi)$.

§ We denote by $\mathbb{I}$ — the identity operator and by $\mathcal{I}$ — the identity superoperator.

strategy, e.g. projection measurement in the eigenbasis of the SLD, for which bounds (1) and (2) coincide. Hence, as in the classical case, the saturability of (2) is guaranteed, but again only in the $k\to\infty$ limit.

2.3. Purification-based definition of QFI

For pure states, $\rho_\varphi = |\psi_\varphi\rangle\langle\psi_\varphi|$, the QFI in (2) simplifies to $F_{\mathrm{Q}}[|\psi_\varphi\rangle] = 4\left(\left\langle\dot\psi_\varphi|\dot\psi_\varphi\right\rangle - \left|\left\langle\dot\psi_\varphi|\psi_\varphi\right\rangle\right|^2\right)$ ‖. Yet, as indicated by (3), for general mixed states the computation of QFI involves diagonalisation of ρ_φ which may be infeasible when dealing with large systems. That is why, it is often necessary to look for upper bounds on QFI that would be efficiently calculable even at the expense of saturability. For this purpose, definitions of QFI were proposed that do not involve computing the SLD, but are specified at the level of state purifications: $\rho_\varphi = \mathrm{Tr}_{\mathrm{E}}\{|\Psi(\varphi)\rangle\langle\Psi(\varphi)|\}$. In [38] the QFI of any ρ_φ has been proven to be equal to the smallest QFI of its purifications $|\Psi(\varphi)\rangle$ ¶:

$$F_{\mathrm{Q}}[\rho_\varphi] = \min_{\Psi(\varphi)} F_{\mathrm{Q}}[|\Psi(\varphi)\rangle] = 4\min_{\Psi(\varphi)}\left\{\left\langle\dot\Psi(\varphi)|\dot\Psi(\varphi)\right\rangle - \left|\left\langle\dot\Psi(\varphi)|\Psi(\varphi)\right\rangle\right|^2\right\}. \tag{4}$$

Independently, in [35] another purification-based QFI definition has been constructed:

$$F_{\mathrm{Q}}[\rho_\varphi] = 4\min_{\Psi(\varphi)}\left\langle\dot\Psi(\varphi)|\dot\Psi(\varphi)\right\rangle. \tag{5}$$

Despite apparent difference, Eqs. (4) and (5) are equivalent and one can prove that any purification minimizing one of them is likewise optimal for the other and satisfies the condition $\left|\dot\Psi(\varphi)\right\rangle = \frac{1}{2}L^{\mathrm{S}}[\rho_\varphi]\otimes\mathbb{I}_{\mathrm{E}}\,|\Psi(\varphi)\rangle$ causing the second term of (4) to vanish. Although for any suboptimal $\Psi(\varphi)$ (4) must provide a strictly tighter bound on QFI than (5), the latter definition, owing to its elegant form, allows for more agility in the minimization procedure, so that it has been efficiently utilized in [35, 39] and is also the base for this paper.

2.4. RLD-based upper bound on QFI

On the other hand, a natural way to construct a bound on QFI and avoid the SLD computation is to relax the Hermiticity condition of the logarithmic derivative. If a non-Hermitian $L[\rho_\varphi]$ satisfying $\partial_\varphi\rho_\varphi = \frac{1}{2}\left(\rho_\varphi L[\rho_\varphi] + L[\rho_\varphi]^\dagger\rho_\varphi\right)$ can be found, as proven in [62, 64], an upper limit on QFI in (2) is obtained: $F_{\mathrm{Q}}[\rho_\varphi] \le \mathrm{Tr}\left\{\rho_\varphi L[\rho_\varphi]L[\rho_\varphi]^\dagger\right\}$. In particular, if and only if $\partial_\varphi\rho_\varphi$ is contained within the support of ρ_φ, one can construct the *Right Logarithmic Derivative* (RLD) by setting $L[\rho_\varphi] = L^{\mathrm{R}}[\rho_\varphi] = \rho_\varphi^{-1}\,\partial_\varphi\rho_\varphi$ and formulate an upper bound on QFI of a simpler form:

$$F_{\mathrm{Q}}[\rho_\varphi] \le F_{\mathrm{Q}}^{\mathrm{RLD}}[\rho_\varphi] = \mathrm{Tr}\left\{\rho_\varphi^{-1}\,(\partial_\varphi\rho_\varphi)^2\right\}. \tag{6}$$

‖ We shorten the notation of functions and superoperators of pure states, so that $F[|\psi\rangle] \equiv F[|\psi\rangle\langle\psi|]$ and $\Lambda[|\psi\rangle] \equiv \Lambda[|\psi\rangle\langle\psi|]$.

¶ See also an alternative formulation based on the convex roof formula, which is valid for unitary parameter estimation [65, 66].

Although (6) is tight only when $L^{\mathrm{R}}[\rho_\varphi] = L^{\mathrm{S}}[\rho_\varphi]$, it still allows to quantify precision well for channel estimation tasks [37], as described in the following section. Lastly, one should note that we are not considering here multi-parameter estimation schemes, for which the RLD may sometimes provide tighter bounds than the SLD [67, 68].

3. Estimation of a quantum channel

3.1. Channel QFI

As in metrological setups the estimated parameter is encoded in the evolution of a system, we identify $\rho_\varphi = \Lambda_\varphi[\rho_{\mathrm{in}}]$ as the final state of a system that started from an input ρ_{in}. The preparation of ρ_{in} is controlled in order to achieve the most precise estimate of φ that parametrizes some general *channel* — a *Completely Positive Trace Preserving* (CPTP) map Λ_φ [59, 60]. Although the form of Λ_φ in general strongly depends on the model considered, the Quantum Cramér-Rao bound always applies, so that precision is upper bounded according to (2) with QFI $F_{\mathrm{Q}}[\Lambda_\varphi[\rho_{\mathrm{in}}]]$. Furthermore, as the QFI is a convex quantity [69], one should restrict oneself to pure input states when seeking the optimal one. Hence, as shown in Figure 2**a**, we define the *channel QFI* as the maximal QFI after performing the input optimisation, so that it has a concrete operational and application-like interpretation:

$$\mathcal{F}[\Lambda_\varphi] = \max_{\psi_{\mathrm{in}}} F_{\mathrm{Q}}[\,\Lambda_\varphi[|\psi_{\mathrm{in}}\rangle]]. \tag{7}$$

For instance, while estimating the duration of the evolution ($\varphi \equiv t$) in an ideal, decoherence-free setting, the CPTP map is unitary leading to a pure channel output. Thus, $\Lambda_\varphi[|\psi_{\mathrm{in}}\rangle] = \mathcal{U}_t[|\psi_{\mathrm{in}}\rangle] = \mathrm{e}^{-\mathrm{i}Ht}\,|\psi_{\mathrm{in}}\rangle\langle\psi_{\mathrm{in}}|\,\mathrm{e}^{\mathrm{i}Ht}$ with H being the Hamiltonian of the evolution. Hence, the definition (7) corresponds to

$$\mathcal{F}[\mathcal{U}_t] = \max_{\psi_{\mathrm{in}}} F_{\mathrm{Q}}\big[\mathrm{e}^{-\mathrm{i}Ht}|\psi_{\mathrm{in}}\rangle\big] = 4\max_{\psi_{\mathrm{in}}}\big\{\langle\psi_{\mathrm{in}}|H^2|\psi_{\mathrm{in}}\rangle - \langle\psi_{\mathrm{in}}|H|\psi_{\mathrm{in}}\rangle^2\big\} = 4\max_{\psi_{\mathrm{in}}}\Delta^2 H, \tag{8}$$

and the optimal states are the ones that maximize the Hamiltonian variance. Note also that in this case the Quantum Cramér-Rao bound takes the form of the time-energy uncertainty relation, $\Delta H\cdot\Delta\tilde{t} \geq 1/2$ [70, 71], with $\Delta\tilde{t}$ being the uncertainty in the estimated duration.

3.2. Purification-based definition of channel QFI

In order to employ the definition (5), we utilize the Stinespring theorem [60] and express the channel Λ_φ as a unitary map U_φ^{SE} on the system combined with an environment disregarded after the evolution. In this way, the output state and its purification respectively read $\Lambda_\varphi[|\psi_{\mathrm{in}}\rangle] = \mathrm{Tr}_{\mathrm{E}}\{|\Psi(\varphi)\rangle\langle\Psi(\varphi)|\}$ and $|\Psi(\varphi)\rangle = U_\varphi^{\mathrm{SE}}\,|\psi_{\mathrm{in}}\rangle\otimes|1\rangle$, where $|1\rangle$ is an arbitrary fixed state chosen to be the first vector in the basis $\{|i\rangle\}_{i=1}^{r}$ of the environment Hilbert space $\mathcal{H}_{\mathrm{E}}^{r}$. By specifying the dimension r of $\mathcal{H}_{\mathrm{E}}^{r}$ to be equal to the rank of Λ_φ, we can generate all non-trivial purifications, $\tilde{\Psi}(\varphi)$, by applying a fictitious, possibly φ-dependent unitary rotation, u_φ^{E}, to the environment, so that

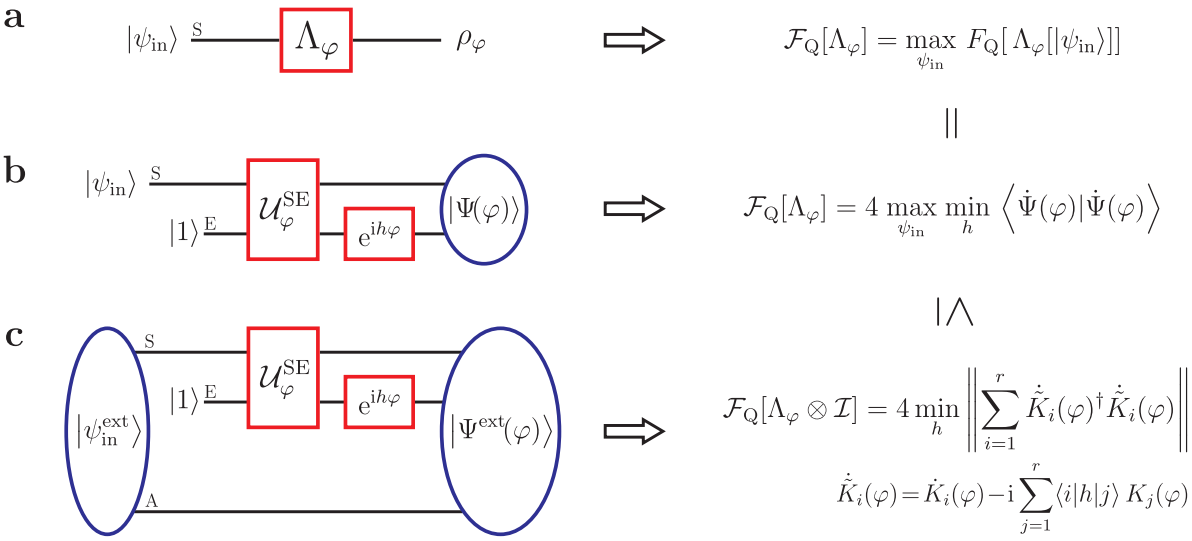

Figure 2. Channel QFI based on the output state purification
(**a**) Channel QFI as the QFI of the output state maximized over all pure input states.
(**b**) Channel QFI obtained from the output state purification generated by a local, fictitious, parameter-dependent environment rotation.
(**c**) Extended channel QFI independent of the maximization over the input states. The environment rotation corresponds to a choice of Kraus representation of the channel.

$\left|\tilde\Psi(\varphi)\right\rangle = \tilde U_\varphi^{\rm SE}\,|\psi_{\rm in}\rangle\otimes|1\rangle$ with $\tilde U_\varphi^{\rm SE} = u_\varphi^{\rm E}\,U_\varphi^{\rm SE}$. Furthermore, writing the channel action in its Kraus representation form $\Lambda_\varphi[|\psi_{\rm in}\rangle] = \sum_{i=1}^r \tilde K_i(\varphi)\,|\psi_{\rm in}\rangle\langle\psi_{\rm in}|\,\tilde K_i(\varphi)^\dagger$, we can identify the Kraus operators corresponding to $\tilde\Psi(\varphi)$ as

$$\tilde K_i(\varphi) = \langle i|\,\tilde U_\varphi^{\rm SE}\,|1\rangle = \sum_{j=1}^r u_{\varphi,ij}^{\rm E}\,K_j(\varphi), \tag{9}$$

where $u_{\varphi,ij}^{\rm E} = \langle i|\,u_\varphi^{\rm E}\,|j\rangle$ and $K_j(\varphi) = \langle j|\,U_\varphi^{\rm SE}\,|1\rangle$ are the Kraus operators of the original purification $\Psi(\varphi)$. Hence, by picking an environment unitary rotation $u_\varphi^{\rm E}$, we are, equivalently to the purification choice, specifying a Kraus representation of Λ_φ. Moreover, as the QFI is a local quantity, we can restrict ourselves to infinitesimal rotations, $u_\varphi^{\rm E} = e^{-ih(\varphi-\varphi_0)}$, in the vicinity of the real value φ_0 that are generated by some Hermitian h. Taking without loss of generality $\varphi_0 = 0$, we obtain the channel version of (5) shown in Figure 2**b** as

$$\mathcal{F}[\Lambda_\varphi] = 4 \max_{\psi_{\rm in}} \min_h \langle\dot{\tilde\Psi}(\varphi)|\dot{\tilde\Psi}(\varphi)\rangle = 4 \max_{\psi_{\rm in}} \min_h \langle\psi_{\rm in}|\sum_{i=1}^r \dot{\tilde K}_i(\varphi)^\dagger \dot{\tilde K}_i(\varphi)|\psi_{\rm in}\rangle, \tag{10}$$

where $|\dot{\tilde\Psi}(\varphi)\rangle = (\dot U_\varphi^{\rm SE} - ihU_\varphi^{\rm SE})|\psi_{\rm in}\rangle\otimes|1\rangle$ and similarly $\dot{\tilde K}_i(\varphi) = \dot K_i(\varphi) - i\sum_{j=1}^r h_{ij}K_j(\varphi)$ with $h_{ij} = \langle i|\,h\,|j\rangle$ being the elements of the generator of Kraus representation rotations (9). Crucially, Figure 2**b** and Equation (10) indicate that the optimal purification/Kraus representation corresponds to the choice of an artificial environment that rotates locally with φ hindering as much as possible information about the estimated parameter.

In order to make the reader familiar with the above formalism, we apply the definition (10) to the previously mentioned case of the evolution duration estimation $\mathcal{U}_t[|\psi_{\rm in}\rangle]$. As the evolution is unitary and $r=1$, the environment/Kraus rotations correspond just to a phase variation $u_t^{\rm E}=\mathrm{e}^{-\mathrm{i}h\,t}$ with h being a real scalar. Hence, (10) simplifies to (8) as expected:

$$\mathcal{F}[\mathcal{U}_t]=4\max_{\psi_{\rm in}}\min_{h}\big\{\langle\psi_{\rm in}|H^2|\psi_{\rm in}\rangle-2h\,\langle\psi_{\rm in}|H|\psi_{\rm in}\rangle+h^2\big\}=4\max_{\psi_{\rm in}}\,\Delta^2 H \tag{11}$$

with minimum occurring at $h=\langle\psi_{\rm in}|H|\psi_{\rm in}\rangle$. Consistently, we would also arrive at (8), if we had used the other QFI purification-based definition (4) as shown in [38].

3.3. Extended channel QFI

The channel QFI (7) is affected by any φ-variations in the form of Λ_φ, quantifying the distinguishability between maps Λ_φ and $\Lambda_{\varphi+\delta\varphi}$. However, any such disturbance may be noticeable only for input states which lead to a measurable change of the channel output that is at best in some "orthogonal direction". As a consequence, the quantity $\min_h\{\ldots\}$ in (10) depends strongly on the pure input $\psi_{\rm in}$, as the minimum occurs for Kraus operators $\big\{K_i^{\rm opt}(\varphi)\big\}_{i=1}^r$ which fulfill the condition $\dot{K}_i^{\rm opt}(\varphi)\,|\psi_{\rm in}\rangle=\frac{1}{2}L^{\rm S}[\Lambda_\varphi\,[|\psi_{\rm in}\rangle]]\;K_i^{\rm opt}(\varphi)\,|\psi_{\rm in}\rangle$ required for the purification of (4) and (5) to be optimal. Maximization of this quantity over $|\psi_{\rm in}\rangle$ is difficult in general, due to the impossibility of exchanging the order of max and min in (10) [35].

Yet, one may construct a natural upper bound on the channel QFI (7) by *extending* the input space, $\mathcal{H}_{\rm S}$, by an equally-large auxiliary space, $\mathcal{H}_{\rm A}$, which is unaffected by the map and measured along with the channel output (see Figure 2**c**). This way, by employing extended input states entangled between these two spaces, $|\psi_{\rm in}^{\rm ext}\rangle\in\mathcal{H}_{\rm S}\times\mathcal{H}_{\rm A}$, one may acquire full available information about φ imprinted by the map Λ_φ on the extended output state. The analogue of (10) defines then the *extended channel QFI* [35]:

$$\mathcal{F}[\Lambda_\varphi\otimes\mathcal{I}]=4\max_{\rho_{\rm in}^{\rm S}}\min_{h}\;\mathrm{Tr}_{\rm S}\left\{\rho_{\rm in}^{\rm S}\sum_{i=1}^{r}\dot{\tilde{K}}_i(\varphi)^\dagger\dot{\tilde{K}}_i(\varphi)\right\}=4\min_{h}\left\|\sum_{i=1}^{r}\dot{\tilde{K}}_i(\varphi)^\dagger\dot{\tilde{K}}_i(\varphi)\right\|, \tag{12}$$

where $\|\ldots\|$ represents the operator norm. The first expression is obtained by tracing over the auxiliary space $\mathcal{H}_{\rm A}$, what leads to the maximisation over all mixed states $\rho_{\rm in}^{\rm S}=\mathrm{Tr}_{\rm A}\{|\psi_{\rm in}^{\rm ext}\rangle\langle\psi_{\rm in}^{\rm ext}|\}$. However, this is exactly (10) with the pure input state replaced by a general mixed one, in which case the order of max and min can be swapped [35] [+]. Consistently, if the optimal input state of (12) is pure, (10) and (12) become equivalent manifesting the uselessness of entanglement between $\mathcal{H}_{\rm S}$ and $\mathcal{H}_{\rm A}$ and irrelevance of the auxiliary space.

Importantly, the extended channel QFI (12) can always be efficiently evaluated numerically by means of semi-definite programming [39] and we show that this is a special case of a more general task of bounding N-parallel channels QFI, as explained

[+] We should stress that (12) *does not* correspond to the situation of using *mixed* states as inputs for *unextended* channel, as mixed states never outperform pure state inputs due to convexity of the QFI.

in Appendix E. For phase estimation schemes with relevant noise models including: *dephasing*, *depolarization*, *loss* and *spontaneous emission*; we determine analytically both (10) and (12) to verify if the use of extended, entangled input states may improve estimation at the single channel level. The corresponding unextended/extended channel QFIs are presented in Table 1, whereas the optimal purifications yielding the minimum of (12) can be found in Appendix A along with the details of the channels considered. The results justify that extension enhances the precision only for depolarization and spontaneous emission channels, for which the input states maximally entangled between $\mathcal{H}_{\mathrm{S}}$ and $\mathcal{H}_{\mathrm{A}}$ are optimal.

3.4. RLD-based upper bound on extended channel QFI

In [37] the applicability of the RLD-based bound (6) has been addressed in the context of channels. By defining the *Choi-Jamiołkowski* (C-J) *representation* [60] of a particular map Λ_φ as $\Omega_{\Lambda_\varphi} = \Lambda_\varphi \otimes \mathcal{I}\left[|\mathbb{I}\rangle\right]$ with $|\mathbb{I}\rangle = \sum_{i=1}^{\dim \mathcal{H}_{\mathrm{S}}} |i\rangle \otimes |i\rangle$, it has been proven that the extended channel QFI can be further upper-bounded by

$$\mathcal{F}[\Lambda_\varphi \otimes \mathcal{I}] \leq \mathcal{F}^{\mathrm{RLD}}[\Lambda_\varphi \otimes \mathcal{I}] = \left\| \mathrm{Tr}_{\mathcal{A}} \left\{ \dot{\Omega}_{\Lambda_\varphi} \Omega_{\Lambda_\varphi}^{-1} \dot{\Omega}_{\Lambda_\varphi} \right\} \right\|, \tag{13}$$

where $\|\ldots\|$ is again the operator norm and $\Omega_{\Lambda_\varphi}^{-1}$ is the inverse of Ω_{Λ_φ} restricted only to the support of the C-J matrix. Most importantly, the bound (13) is determined solely by the form of Λ_φ, i.e. its C-J representation, and does not contain any extra information about the space of input states accepted by the map. This contrasts the definitions of purification-based unextended/extended channel QFIs (10)/(12) and facilitates the analyticity of the results presented in Table 1. On the other hand, as indicated in Section 2.4, both applicability and tightness of the RLD-based bounds are limited. The bound (13) is valid only when $\dot{\Omega}^2_{\Lambda_\varphi}$ is fully supported by Ω_{Λ_φ} [37]. However, we give an intuitive reason for this restriction by proving that this condition is equivalent (see Appendix B) to the notion of channel Λ_φ being *φ-non-extremal*, as introduced in [39] and also revisited in the following section. This confirms that the exclusive dependence of (13) on Ω_{Λ_φ} has indeed a strong geometrical meaning. Moreover, although the RLD-based bounds depicted in Table 1 for the relevant channels seem to be far above the corresponding channel QFIs — (7) and (12), they are of great significance. The bound (13) is additive for any maps $\Lambda_\varphi^{(1)}$, $\Lambda_\varphi^{(2)}$ to which it applies [37], thus

$$\begin{aligned} &\mathcal{F}^{\mathrm{RLD}}\left[\left(\Lambda_\varphi^{(1)} \otimes \mathcal{I}\right) \otimes \left(\Lambda_\varphi^{(2)} \otimes \mathcal{I}\right)\right] = \mathcal{F}^{\mathrm{RLD}}\left[\Lambda_\varphi^{(1)} \otimes \mathcal{I}\right] + \mathcal{F}^{\mathrm{RLD}}\left[\Lambda_\varphi^{(2)} \otimes \mathcal{I}\right] \\ &\therefore \quad \mathcal{F}\left[\left(\Lambda_\varphi \otimes \mathcal{I}\right)^{\otimes N}\right] \leq \mathcal{F}^{\mathrm{RLD}}\left[\left(\Lambda_\varphi \otimes \mathcal{I}\right)^{\otimes N}\right] = N\, \mathcal{F}^{\mathrm{RLD}}[\Lambda_\varphi \otimes \mathcal{I}]\,. \end{aligned} \tag{14}$$

Hence, it constrains not only the QFI of a single extended channel, but also restricts the QFI of N extended channels used in parallel to scale at most linearly with N. Crucially, as the extension can only improve the precision, (14) is also a valid upper-bound on the QFI of N uses of an unextended channel, which asymptotic precision scaling is then limited to a constant factor improvement over the SQL (see Section 4.1).

Noise model	$\mathcal{F}[\Lambda_\varphi]$	$\mathcal{F}[\Lambda_\varphi \otimes \mathcal{I}]$	$\mathcal{F}_{\text{as}}^{\text{CE}}$ in [39]	$\mathcal{F}_{\text{as}}^{\text{QS}}$	$\mathcal{F}^{\text{RLD}}[\Lambda_\varphi \otimes \mathcal{I}]$	$\mathcal{F}_{\text{as}}^{\text{CS}}$ in [39]
Dephasing	η^2	η^2	$\frac{\eta^2}{1-\eta^2}$	$\frac{\eta^2}{1-\eta^2}$	$\frac{\eta^2}{1-\eta^2}$	$\frac{\eta^2}{1-\eta^2}$
Depolarization	η^2	$\frac{2\eta^2}{1+\eta}$	$\frac{2\eta^2}{(1-\eta)(1+2\eta)}$	$\frac{2\eta^2}{(1-\eta)(1+2\eta)}$	$\frac{2\eta^2(1+\eta)}{(1-\eta)(1+3\eta)}$	$\frac{4\eta^2}{(1-\eta)(1+3\eta)}$
Loss	η	η	$\frac{\eta}{1-\eta}$	$\frac{\eta}{1-\eta}$	n.a.	n.a.
Spontaneous emission	η	$\frac{4\eta}{\left(1+\sqrt{\eta}\right)^2}$	$\frac{4\eta}{1-\eta}$	n.a.	n.a.	n.a.

Table 1. Channel phase estimation sensitivity quantified via QFIs and their asymptotic bounds. Noise models of metrological relevance discussed in the paper are listed in the first column. Decoherence strength increases with a decrease of the η parameter ($0 \leq \eta < 1$) (see Appendix A for details). From left to right — single channel QFI; extended channel QFI; upper bounds on asymptotic channel QFI (16) in ascending order: channel extension bound (see Section 4.1.3), quantum simulation bound (see Section 4.1.2), RLD-based bound (see Section 3.4), classical simulation bound (see Section 4.1.1). [n.a. — not available]

4. Estimation of N independent quantum channels

In order to describe general metrological schemes depicted in Figure 1**a**, we model the evolution of all particles within the probe as N identical, independent channels acting on a possibly entangled, pure input state of the whole probe $\left|\psi_{\text{in}}^N\right\rangle$. The final output state of the probe then reads $\rho_\varphi^N = \Lambda_\varphi^{\otimes N}\left[\left|\psi_{\text{in}}^N\right\rangle\right]$ yielding the *N-channel QFI*:

$$\mathcal{F}\left[\Lambda_\varphi^{\otimes N}\right] = \max_{\psi_{\text{in}}^N} F_{\text{Q}}\left[\,\Lambda_\varphi^{\otimes N}\left[\left|\psi_{\text{in}}^N\right\rangle\right]\right], \tag{15}$$

which linear or quadratic dependence on N dictates respectively the SQL or HL scaling of precision. For example, when considering classical schemes that employ unentangled probes, $\left|\psi_{\text{in}}^N\right\rangle = \otimes_{n=1}^N \left|\psi_{\text{in}}^1\right\rangle$, we are effectively dealing with N independent subsystems, so that $\mathcal{F}\left[\Lambda_\varphi^{\otimes N}\right] = N\,\mathcal{F}[\Lambda_\varphi]$ and the uncertainty of the estimate $\tilde{\varphi}$ decreases as $1/\sqrt{N}$.

4.1. SQL-like bounds on precision in the asymptotic N limit

To investigate channels that incorporate the uncorrelated noise restricting the asymptotic precision scaling to SQL, we define the *asymptotic channel QFI* as

$$\mathcal{F}_{\text{as}}[\Lambda_\varphi] = \lim_{N\to\infty} \frac{\mathcal{F}\left[\Lambda_\varphi^{\otimes N}\right]}{N}. \tag{16}$$

Thus, for such SQL-bound channels, (16) is finite and $\mathcal{F}_{\text{as}}[\Lambda_\varphi] \geq \mathcal{F}[\Lambda_\varphi]$ with equality indicating the optimality of classical estimation schemes. Hence, (16) quantifies the *maximal quantum precision enhancement* that reads

$$\chi[\Lambda_\varphi] = \lim_{N\to\infty} \frac{\Delta\tilde{\varphi}_{\text{cl}}}{\Delta\tilde{\varphi}_{\text{Q}}} = \sqrt{\frac{\mathcal{F}_{\text{as}}[\Lambda_\varphi]}{\mathcal{F}[\Lambda_\varphi]}} \geq 1. \tag{17}$$

However, as the computation of (16) is generally infeasible owing to the complexity of QFI rising exponentially with N, one normally needs to construct an upper limit on the N-channel QFI (15), $\mathcal{F}^{\text{bound}}[\Lambda_\varphi^{\otimes N}]$, from which the asymptotic form, $\mathcal{F}_{\text{as}}^{\text{bound}}$, may be constructed using (16) that upper-bounds both the N-channel QFI and the maximal quantum precision enhancement:

$$\mathcal{F}\big[\Lambda_\varphi^{\otimes N}\big] \leq N\,\mathcal{F}_{\text{as}}^{\text{bound}}, \qquad\qquad \chi[\Lambda_\varphi] \leq \sqrt{\frac{\mathcal{F}_{\text{as}}^{\text{bound}}[\Lambda_\varphi]}{\mathcal{F}[\Lambda_\varphi]}}. \tag{18}$$

Methods of constructing $\mathcal{F}_{\text{as}}^{\text{bound}}$ were proposed in [39] basing on the concepts of channel *classical simulation* (CS) and *channel extension* (CE). As mentioned already, the CS method applies only to *φ-non-extremal* channels, for which also the RLD-based bound (14) provides a valid example of $\mathcal{F}_{\text{as}}^{\text{bound}}$. Yet, the notion of CS may be generalized to the idea of channel *quantum simulation* (QS) introduced in [36], in order to obtain an asymptotic bound applicable to a wider class of quantum maps. All these four approaches ($\mathcal{F}_{\text{as}}^{\text{bound}} = \mathcal{F}_{\text{as}}^{\text{CS}}, \mathcal{F}_{\text{as}}^{\text{CE}}, \mathcal{F}^{\text{RLD}}[\Lambda_\varphi\otimes\mathcal{I}]\,, \mathcal{F}_{\text{as}}^{\text{QS}}$ respectively) are presented in Table 1 on the right hand side of the double-line for the relevant channels. As the lossy and spontaneous emission interferometry cases are examples of φ-extremal maps, they do not allow for $\mathcal{F}_{\text{as}}^{\text{CS}}$ and $\mathcal{F}^{\text{RLD}}[\Lambda_\varphi\otimes\mathcal{I}]$ to be constructed. In the case of depolarization channel, which is full-rank [60] and hence φ-non-extremal, despite the lack of a simple geometric interpretation of its value, $\mathcal{F}^{\text{RLD}}[\Lambda_\varphi\otimes\mathcal{I}]$ proves to be tighter than $\mathcal{F}_{\text{as}}^{\text{CS}}$. The more general QS approach not only applies also to the (φ-extremal) lossy interferometry case, but also provides as accurate bounds as the CE method. Nevertheless, as the CE approach is proven to provide at least as tight bounds for the broadest class of quantum channels containing ones to which the other methods apply, we use it to quantify the maximal quantum precision enhancements (17) for the channels considered (see Table 2). Below, we describe alternately the CS, QS and CE methods — ordered according to their power and generality.

4.1.1. Classical Simulation method

As introduced in [36] and depicted in Figure 1**b**, a channel admits a *classical simulation* (CS) of itself, if for any ϱ it is expressible in the form

$$\Lambda_\varphi[\varrho] = \Phi[\varrho\otimes p_\varphi] = \sum_i p_{\varphi,i}\,\Pi_i[\varrho]\,, \tag{19}$$

where $p_\varphi = \sum_i p_{\varphi,i}\,|e_i\rangle\langle e_i|$ is a classical, diagonal density matrix in some basis and Φ is a φ-independent CPTP map acting on a larger input space. By defining $\Pi_i[\varrho] = \Phi[\varrho\otimes|e_i\rangle\langle e_i|]$ one obtains the second equality in (19), so that it becomes evident that the estimated φ parametrizes only the mixing probabilities of some φ-independent quantum maps. Then, the N-channel QFI (15) can be simply upper-bounded via $\mathcal{F}\big[\Lambda_\varphi^{\otimes N}\big] \leq N\,F_{\text{cl}}[p_{\varphi,i}]$, where $F_{\text{cl}}[p_{\varphi,i}]$ is the discrete version of classical FI in (1) and plays the role of $\mathcal{F}_{\text{as}}^{\text{bound}}$ in (18) [36, 39]. Moreover, as QFI is a local quantity, in order to construct a CS-based $\mathcal{F}_{\text{as}}^{\text{bound}}$ valid for small deviations $\delta\varphi$ around a given φ, the classical simulation must be feasible only locally, i.e. $\Lambda_\varphi[\varrho] = \sum_i p_{\varphi,i}\,\Pi_i[\varrho] + O(\delta\varphi^2)$. Therefore,

as proven in [36], if the C-J representation Ω_{Λ_φ} of a channel Λ_φ allows for parameters $\epsilon_\pm > 0$ such that the matrices $\Omega_{\Pi_\pm} = \Omega_{\Lambda_\varphi} \pm \epsilon_\pm \dot{\Omega}_{\Lambda_\varphi}$ are positive semi-definite at a given φ, the channel is *φ-non-extremal* there and the necessary $p_{\varphi,i}$ can always be found. This is because one can construct $\Omega_{\tilde{\Lambda}_\varphi} = p_{\varphi,+}\Omega_{\Pi_+} + p_{\varphi,-}\Omega_{\Pi_-}$ that up to $O(\delta\varphi^2)$ coincides with Ω_{Λ_φ} by choosing $p_{\varphi,\pm}$ such that $\Omega_{\tilde{\Lambda}_\varphi} = \Omega_{\Lambda_\varphi}$ and $\dot{\Omega}_{\tilde{\Lambda}_\varphi} = \dot{\Omega}_{\Lambda_\varphi}$. Hence, $\Lambda_\varphi[\varrho] = \tilde{\Lambda}_\varphi[\varrho] + O(\delta\varphi^2)$ with $\tilde{\Lambda}_\varphi[\varrho] = p_{\varphi,+}\Pi_+ + p_{\varphi,-}\Pi_-$, so that $F_{\rm cl}[p_{\varphi,\pm}] = 1/(\epsilon_+\epsilon_-)$ is a legal example of the required bound valid at φ. Furthermore, in [39], it has been proven that for channels of the form $\Lambda_\varphi[\varrho] = \Lambda[\mathcal{U}_\varphi[\varrho]]$ this two-point construction is always optimal at any φ when maximal possible $\epsilon_\pm$ are chosen *. Geometrically, imagining the convex set of all CPTP maps in their C-J representation that share input and output spaces of Λ_φ, the channels $\Omega_{\Pi_\pm}$ lie at the intersection points of the tangent generated by $\dot{\Omega}_{\Lambda_\varphi}$ at Ω_{Λ_φ} and the boundary of the set. The $\mathcal{F}_{\rm as}^{\rm bound}$ of (18), which we refer to as the *asymptotic CS bound* — $\mathcal{F}_{\rm as}^{\rm CS} = 1/(\epsilon_+^{\rm max}\epsilon_-^{\rm max})$, is dictated then by the "distances" $\epsilon_\pm^{\rm max}$ of the channel to the boundary measured along this tangent. Although the CS approach provides weaker bounds than the CE method [39], it gives an intuitive geometric explanation of the inevitable asymptotic SQL-like scaling of all φ-non-extremal maps. These naturally include the full-rank channels [60], which lie inside the set of CPTP maps away from its boundary.

4.1.2. Quantum Simulation method

In [36], a natural generalization of the channel CS has been proposed which is schematically presented in Figure 1**b**. This, so called, *quantum simulation* (QS) of a channel corresponds to expressing its action in a form similar to (19) that reads

$$\Lambda_\varphi[\varrho] = \Phi[\varrho \otimes \sigma_\varphi] = {\rm Tr}_{{\rm E}_\Phi {\rm E}_\sigma}\Big\{ U \left(\varrho \otimes |\psi_\varphi\rangle_{{\rm E}_\Phi {\rm E}_\sigma}\langle\psi_\varphi| \right) U^\dagger \Big\}, \tag{20}$$

where now σ_φ is a quantum, non-diagonal, φ-dependent density matrix, and the purified form on the right hand side involves both channel Φ environment space ${\rm E}_\Phi$ as well as σ_φ purification space ${\rm E}_\sigma$ such that $\sigma_\varphi = {\rm Tr}_{{\rm E}_\sigma}\{|\psi_\varphi\rangle\langle\psi_\varphi|\}$. Note that the notion of quantum simulability is equivalent to the *channel programmability* concept introduced in [34]. Following the same argumentation as in [39] for CS, the N-channel QFI (15) of a quantum simulable channel can be linearly bounded as $\mathcal{F}\big[\Lambda_\varphi^{\otimes N}\big] \leq N\, F_{\rm Q}[\sigma_\varphi]$, and therefore the asymptotic bound reads $\mathcal{F}_{\rm as}^{\rm bound} = F_{\rm Q}[\sigma_\varphi]$. Similarly to CS, a channel may admit many decompositions (20) and the optimal one must yield the lowest $F_{\rm Q}[\sigma_\varphi]$. Therefore, without loss of generality, in the search for the optimal QS, we may take U in (20) to act on the full purified system, i.e. also in ${\rm E}_\Phi$ and ${\rm E}_\sigma$ spaces. This enlarges the set of all possible QSs beyond the original ones $U = U^{{\rm SE}_\Phi} \otimes \mathbb{I}^{{\rm E}_\sigma}$ and yields $\mathcal{F}_{\rm as}^{\rm bound} = F_{\rm Q}[|\psi_\varphi\rangle]$, which via (4) cannot be smaller than $F_{\rm Q}[\sigma_\varphi]$. In fact, (4) assures that for any QS employing σ_φ, there exists an "enlarged" decomposition (20) leading to the same $\mathcal{F}_{\rm as}^{\rm bound}$ with $|\psi_\varphi\rangle$ being the minimal purification in (4). In conclusion, we may seek the optimal QS by analysing all possible decompositions of the form (20) that, owing

* Yet, it may prove optimal for channels of other type, as shown for transversal dephasing in [40].

to the locality of the QFI, must be feasible only for small deviations $\delta\varphi$ from a given φ, so that $\Lambda_\varphi[\varrho] = \mathrm{Tr}_{\mathrm{E}\Phi\mathrm{E}_\sigma}\{U\,(\varrho\otimes|\psi_\varphi\rangle\langle\psi_\varphi|)\,U^\dagger\} + O(\delta\varphi^2)$. In Appendix D, we prove that, in order for the QS (20) to be possible locally at φ, Λ_φ of rank r must admit Kraus operators $\{K_i(\varphi)\}_{i=1}^r$ that satisfy the two conditions:

$$\mathrm{i}\sum_{i=1}^{r}\dot{K}_i(\varphi)^\dagger K_i(\varphi) = 0 \qquad \text{and} \qquad \sum_{i=1}^{r}\dot{K}_i(\varphi)^\dagger\dot{K}_i(\varphi) = \frac{1}{4}F_{\mathrm{Q}}[|\psi_\varphi\rangle]\;\mathbb{I}. \tag{21}$$

Hence, by optimizing over all locally equivalent Kraus representations of Λ_φ — the ones related to one another by rotations (9) generated by any Hermitian h — that satisfy constraints (21), we may determine the asymptotic bound given by the optimal local QS, which we refer to as the *asymptotic QS bound* — $\mathcal{F}_{\mathrm{as}}^{\mathrm{QS}}$, as follows

$$\mathcal{F}_{\mathrm{as}}^{\mathrm{QS}} = \min_h \lambda \quad \text{subject to:}\;\; \alpha_{\tilde{K}} = \frac{\lambda}{4}\mathbb{I},\; \beta_{\tilde{K}} = 0, \tag{22}$$

where $\alpha_{\tilde{K}} = \sum_{i=1}^r \dot{\tilde{K}}_i(\varphi)^\dagger\dot{\tilde{K}}_i(\varphi)$, $\beta_{\tilde{K}} = \mathrm{i}\sum_{i=1}^r \dot{\tilde{K}}_i(\varphi)^\dagger\tilde{K}_i(\varphi)$ and λ has the interpretation of $\mathcal{F}_{\mathrm{as}}^{\mathrm{bound}} = F_{\mathrm{Q}}[|\psi_\varphi\rangle]$ for a local QS of the form (20). Before revisiting the CE method explicitly below, we should note that (22) resembles exactly the asymptotic CE bound of [39] with an extra constraint forcing the operator $\alpha_{\tilde{K}}$ to be proportional to identity. This proves that indeed the QS method can never outperform the CE approach.

Investigating the relevant quantum maps considered in Table 1, the QS method must naturally apply to dephasing and depolarization channels. These are φ-non-extremal (classically simulable) maps, hence their locally constructible CSs (19) serve as examples of the more general QSs (20). Consistently, the Kraus representations utilized in [39] to obtain the asymptotic CE bounds for these two channels fulfil the $\alpha_{\tilde{K}} \propto \mathbb{I}$ constraint. Thus, QS is not only feasible in their case but also its asymptotic bound coincides with the one of the superior CE method. Significantly, also in the case of the lossy interferometry the optimal Kraus operators used in [39] to minimize the asymptotic CE bound satisfy the extra QS's constraint. This fact indicates that also for φ-extremal channels QS may prove to be as good as CE. However, in the case of spontaneous emission, the QS method seizes to work, as the $\beta_{\tilde{K}} = 0$ condition fixes $\alpha_{\tilde{K}}$ to be disproportional to identity [39].

4.1.3. Channel Extension method

The *channel extension* (CE) method of [39] not only applies to the widest class of quantum maps containing all φ-non-extremal ones, but also provides more stringent bounds than the CS, RLD and QS equivalents, as respectively proven in [39], Appendix C and above. In this method, see Figure 1**b**, each single channel is extended by an auxiliary ancilla as introduced in Section 3.3. In [35], it has been proven that one can then effectively bound the N-channel QFI (15) via the *N-extended-channel QFI*, so that

$$\mathcal{F}\big[\Lambda_\varphi^{\otimes N}\big] \leq \mathcal{F}\Big[\big(\Lambda_\varphi\otimes\mathcal{I}\big)^{\otimes N}\Big] \leq 4\,\min_h\left\{N\,\|\alpha_{\tilde{K}}\| + N(N-1)\,\|\beta_{\tilde{K}}\|^2\right\}, \tag{23}$$

Noise model	*Dephasing*	*Depolarization*	*Loss*	*Spontaneous emission*
$\chi[\Lambda_\varphi]$	$=\sqrt{\frac{1}{1-\eta^2}}$	$\leq\sqrt{\frac{2}{(1-\eta)(1+2\eta)}}$	$=\sqrt{\frac{1}{1-\eta}}$	$\leq\sqrt{\frac{4}{1-\eta}}$
$\chi[\Lambda_\varphi\otimes\mathcal{I}]$	$=\sqrt{\frac{1}{1-\eta^2}}$	$=\sqrt{\frac{1+\eta}{(1-\eta)(1+2\eta)}}$	$=\sqrt{\frac{1}{1-\eta}}$	$=\sqrt{\frac{1+\sqrt{\eta}}{1-\sqrt{\eta}}}$

Table 2. Quantum phase estimation precision enhancement from the CE method. For all noise models specified in Appendix A, the asymptotic CE bounds on the maximal quantum precision enhancement factors, $\chi[\bullet]=\sqrt{\mathcal{F}_{\rm as}[\bullet]/\mathcal{F}[\bullet]}$, are presented. For a general quantum map Λ_φ, the CE bound only upper-limits $\chi[\Lambda_\varphi]$ as $\mathcal{F}_{\rm as}[\Lambda_\varphi]\leq\mathcal{F}_{\rm as}^{\rm CE}$. Yet, for dephasing and lossy interferometry, as indicated by "=", the corresponding values of $\chi[\Lambda_\varphi]$ have been shown to be attainable [72, 73]. For an extended channel, $\chi[\Lambda_\varphi\otimes\mathcal{I}]$ is determined by the CE bound as $\mathcal{F}_{\rm as}[\Lambda_\varphi\otimes\mathcal{I}]=\mathcal{F}_{\rm as}^{\rm CE}$.

where again $\alpha_{\tilde{K}}=\sum_{i=1}^r\dot{\tilde{K}}_i(\varphi)^\dagger\dot{\tilde{K}}_i(\varphi)$, $\beta_{\tilde{K}}=\mathrm{i}\sum_{i=1}^r\dot{\tilde{K}}_i(\varphi)^\dagger\tilde{K}_i(\varphi)$ and h is the generator of local Kraus representation rotations (9). Crucially, if there exists a Kraus representation for which the second term in (23) vanishes, $\mathcal{F}\left[\Lambda_\varphi^{\otimes N}\right]$ must asymptotically scale linearly in N. This requirement corresponds to the constraint $\beta_{\tilde{K}}=0$ already accounted in the QS method, which for any linearly independent Kraus operators $\{K_i\}_{i=1}^r$ is equivalent to the existence of h such that [35]

$$\sum_{i,j=1}^r h_{ij}\,K_i^\dagger K_j=\mathrm{i}\sum_{i=1}^r\dot{K}_i(\varphi)^\dagger K_i(\varphi). \tag{24}$$

What is more, for any channel that admits an h fulfilling (24), one can show basing on the results of [35] that the second inequality in (23) is saturated in the $N\to\infty$ limit, so that the *asymptotic extended channel QFI* then reads

$$\mathcal{F}_{\rm as}[\Lambda_\varphi\otimes\mathcal{I}]=\lim_{N\to\infty}\frac{\mathcal{F}\left[(\Lambda_\varphi\otimes\mathcal{I})^{\otimes N}\right]}{N}=4\min_{\substack{h\\ \beta_{\tilde{K}}=0}}\left\|\sum_{i=1}^r\dot{\tilde{K}}_i(\varphi)^\dagger\dot{\tilde{K}}_i(\varphi)\right\|. \tag{25}$$

Importantly, (25) becomes the required asymptotic bound $\mathcal{F}_{\rm as}^{\rm bound}$ of (18), which we refer to as the *asymptotic CE bound* — $\mathcal{F}_{\rm as}^{\rm CE}$. We explicitly wrote the full form of (25) to emphasize its similarity to the extended *single* channel QFI (12). The essential difference in (25) is the constraint (24) yielding $\mathcal{F}_{\rm as}[\Lambda_\varphi\otimes\mathcal{I}]\geq\mathcal{F}[\Lambda_\varphi\otimes\mathcal{I}]$ and dictating the maximal quantum precision enhancement for an extended channel:

$$\chi[\Lambda_\varphi\otimes\mathcal{I}]=\lim_{N\to\infty}\frac{\Delta\tilde{\varphi}_{\rm cl}^{\rm ext}}{\Delta\tilde{\varphi}_{\rm Q}^{\rm ext}}=\sqrt{\frac{\mathcal{F}_{\rm as}[\Lambda_\varphi\otimes\mathcal{I}]}{\mathcal{F}[\Lambda_\varphi\otimes\mathcal{I}]}}\geq 1. \tag{26}$$

Similarly to (12), (25) is computable by means of semi-definite programming [39], so that one can efficiently determine both (18) and (26). The CE-based bounds on $\chi[\Lambda_\varphi]$ and the exact values of $\chi[\Lambda_\varphi\otimes\mathcal{I}]$ for the relevant noise models are presented in Table 2. Although generally the CE method only upper-limits the maximal quantum precision enhancement (17), it has been proven to quantify $\chi[\Lambda_\varphi]$ exactly in the case of dephasing

[72] and lossy interferometer channels [73]. This has been achieved by showing that input states utilizing spin- and light- squeezing respectively yield a quantum enhancement that asymptotically attains the corresponding CE-based bounds presented in Table 2. On the other hand, as indicated in Table 1, these channels are also examples of ones for which the extension does not improve the precision at the single channel level, so that $\chi[\Lambda_\varphi]=\chi[\Lambda_\varphi\otimes\mathcal{I}]$ in Table 2. The question — when the lack of precision improvement due to extension at the single channel level translates to the asymptotic regime, i.e $\mathcal{F}[\Lambda_\varphi]=\mathcal{F}[\Lambda_\varphi\otimes\mathcal{I}] \underset{?}{\Longleftrightarrow} \mathcal{F}_{\rm as}[\Lambda_\varphi]=\mathcal{F}_{\rm as}[\Lambda_\varphi\otimes\mathcal{I}]$, we leave open for future research.

4.2. Finite-N Channel Extension method

In Section 4.1, we have presented the CE method as the most effective one out of all discussed that provides the tightest upper limits on the maximal possible asymptotic quantum precision enhancement. On the other hand, in the case of experiments such as optical interferometry with moderate numbers of photons [8, 9], the asymptotic CE bounds, despite still being valid, are far too weak to be useful. For very low values of N, the precision can be quantified numerically, for instance by brute-force type methods computing explicitly the QFI. However, in the intermediate N regime — being beyond the reach of computational power, yet with N too low for the asymptotic methods to be effective — more accurate bounds should play an important role.

We propose the *finite-N channel extension* method, which despite being based on the properties of a single channel, still provides bounds on precision that are relevant in the intermediate N regime. We utilize the upper-limit (23) on the N-extended-channel QFI and construct the *finite-N CE bound*, $\mathcal{F}_N^{\rm CE}$, that reads

$$\frac{\mathcal{F}\Big[(\Lambda_\varphi\otimes\mathcal{I})^{\otimes N}\Big]}{N} \;\leq\; \mathcal{F}_N^{\rm CE}=4\min_h\big\{\|\alpha_{\tilde{K}}\|+(N-1)\,\|\beta_{\tilde{K}}\|^2\big\}. \tag{27}$$

Following the suggestion of [39], in contrast to the asymptotic CE bound $\mathcal{F}_{\rm as}^{\rm CE}$ defined in (25), we do not impose the SQL-bounding condition $\beta_{\tilde{K}}=0$ (24), but we seek at each N for the minimal Kraus representation that is generated by some optimal $h=h_{\rm opt}(N)$ being now not only channel but also N-dependent. Still, as shown in Appendix E, $\mathcal{F}_N^{\rm CE}$ can always be efficiently evaluated numerically by recasting the minimization over h in (27) into a semi-definite programming task. Moreover, as the finite-N CE bound varies smoothly between $N=1$ and $N=\infty$, at which it is tight, it provides more accurate bounds than its asymptotic version. For $N=1$, $\mathcal{F}_N^{\rm CE}$ coincides with the extended channel QFI (12) — $\mathcal{F}_{N=1}^{\rm CE}=\mathcal{F}[\Lambda_\varphi\otimes\mathcal{I}]$, whereas in the $N\to\infty$ limit it attains the asymptotic CE bound (25) — $\mathcal{F}_{N\to\infty}^{\rm CE}=\mathcal{F}_{\rm as}^{\rm CE}$.

What is more, when considering channels for which the asymptotic CE method fails, as it is not possible to set $\beta_{\tilde{K}}=0$ in (23) for any Kraus representation, (27) still applies and it is the finite-N CE method that provides the correct CE-based bound in the $N\to\infty$ limit that in principle may then surpass the SQL-like scaling. On the other hand, when dealing with estimation schemes in which one can moderate the effective

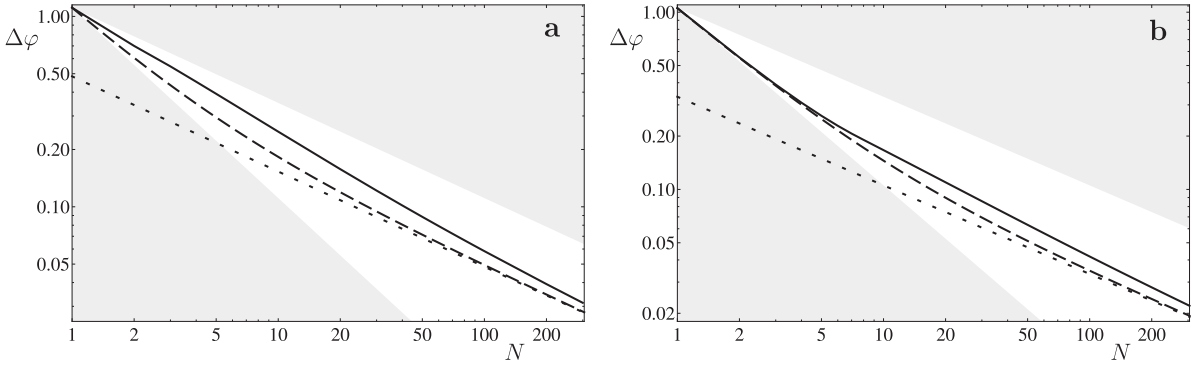

Figure 3. Phase estimation CE method based bounds on precision
(**a**) *Dephasing*: Finite-N (*dashed*) and the asymptotic CE bounds (*dotted*) on estimation uncertainty as compared with the precision achieved by utilizing spin-squeezed states in a Ramsey spectroscopy setup with probe consisting of N atoms experiencing uncorrelated dephasing with $\eta = 0.9$ (*solid*).
(**b**) *Loss*: Lossy interferometry with particle survival probability $\eta = 0.9$, e.g. Mach-Zehnder interferometer experiencing photonic loss in both of its arms, with effective power transmission η. The smallest uncertainty in a phase estimation scheme is quantified by calculating the QFI for numerically optimized N-particle input states. Again, finite-N (*dashed*) and asymptotic CE bounds (*dotted*) on precision are shown for comparison.

amount of loss (i.e. the form of Λ_φ) depending on the number of particles, the asymptotic bound $\mathcal{F}_{\rm as}^{\rm CE}$ may not actually be the tightest within the CE method. The $\beta_{\tilde{K}}$ of (23) and (27) becomes then a function of N and it may not be asymptotically optimal to set it equal to zero by imposing condition (24). Yet, the finite-N CE method being not constrained with $\beta_{\tilde{K}}=0$ still yields the correct CE-based bound on precision as $N\to\infty$. This fact has been utilized in [40], where, owing to the N-dependence of $\beta_{\tilde{K}}$, the finite-N CE method provided an asymptotic bound indeed tighter than the naively calculated $\mathcal{F}_{\rm as}^{\rm CE}$. What is more, the $\mathcal{F}_{N\to\infty}^{\rm CE}$ has been numerically shown there to be saturable, what proves the power of the more agile finite-N CE method. For phase estimation with various decoherence models including dephasing, depolarization, loss and spontaneous emission described in detail in Appendix A, we observe that the finite-N CE bound is simply related to its asymptotic form as

$$\mathcal{F}_N^{\rm CE} = \frac{N\,\mathcal{F}_{\rm as}^{\rm CE}}{N+\mathcal{F}_{\rm as}^{\rm CE}}, \tag{28}$$

where one should substitute for $\mathcal{F}_{\rm as}^{\rm CE}$ the corresponding asymptotic CE bounds presented in Table 1 ♯.

For dephasing and lossy interferometry models, we show explicitly in Figure 3 both the asymptotic and the finite-N bounds accompanied by the plots of actual precision achievable with explicit estimation strategies optimal in the large N regime. In the first case, we consider a Ramsey spectroscopy setup of [13, 14] in which the probe consists

♯ In the case of spontanous emission noise the formula is valid only for $N \geq 2$, what we suspect to be a consequence of the spontaneous emission channel being an extremal map [60].

of atoms prepared in a spin-squeezed state [72]. The parameter is then encoded in the phase of a unitary rotation generated by the total angular momentum of the atoms that simultaneously experience uncorrelated dephasing. After measuring probe's total angular momentum perpendicular to the one generating the estimated phase change, the parameter is reconstructed with uncertainty plotted in Figure 3**a**. In the second lossy interferometry case, each particle is subject to an independent loss process with survival probability η, as in e.g. Mach-Zehnder interferometer with power transmission η in both arms [29, 30]. Here the solid line represents the maximal QFI achieved with numerically optimised N-photon states. Although in this case the maximal quantum enhancement of Table 2 can also be achieved via an estimation strategy that employs squeezed-light as the input with mean number of photons constrained to $N = \bar{N}$ [73], we cannot compare its precision with the one bounded through $\mathcal{F}^{\mathrm{CE}}_{N=\bar{N}}$. As $N\cdot\mathcal{F}^{\mathrm{CE}}_{N}$ is a convex quantity in N, one cannot use it naively to constrain precision after replacing N by the mean number of photons $\bar{N}$. This contrasts the case of the (constant) asymptotic CE bound, which yields $N\cdot\mathcal{F}^{\mathrm{CE}}_{\mathrm{as}}$ being linear in N, so that it also applies to estimation strategies employing states of indefinite photon number, as pointed in [39].

5. Frequency estimation in atomic models

We apply the methods discussed above to the case of frequency estimation problems in atomic spectroscopy. The general Ramsey spectroscopy setup considered in [13, 14, 22–26, 40] corresponds to N identical two-level atoms — spin-1/2 systems — with their states separated, where typically the detuning ω of an external oscillator frequency from the atoms transition frequency is to be estimated. We assume that the full experiment takes an overall time T, during which the estimation procedure is repeated $k = T/t$ times, where t is the evolution duration of each experimental shot. The Quantum Cramér-Rao bound (2) on precision of the estimate $\tilde{\omega}$ can be then conveniently rewritten as

$$\Delta\tilde{\omega} \geq \frac{1}{\sqrt{T\, f_t[\rho^N_\omega(t)]}}\,, \tag{29}$$

where $f_t[\varrho(t)] = F_{\mathrm{Q}}[\varrho(t)]\,/t$ is now the effective QFI per shot duration and $\rho^N_\omega(t)$ denotes the final state of the whole probe containing N particles being measured in each shot. The total time T plays then the role of k in (2) and, after fixing t, the bound (29) can always be saturated as $T \to \infty$. The evolution of the probe can be modelled by the master equation of the Lindblad [54] form

$$\frac{\partial\rho^N_\omega(t)}{\partial t} = \sum_{n=1}^{N} \mathrm{i}\,\frac{\omega}{2}\left[\sigma_3^{(n)}, \rho^N_\omega(t)\right] + \mathcal{L}^{(n)}\left[\rho^N_\omega(t)\right], \tag{30}$$

where $\sigma_3^{(n)}$ is the Pauli operator generating a unitary rotation of the n'th atom around the z axis in its Bloch ball representation. The uncorrelated noise is represented by the Liouvillian part $\mathcal{L}^{(n)}$ acting independently on each, here the n'th, particle, so that effectively $\rho^N_\omega(t) = \Lambda^{\otimes N}_{\omega;t}\left[\left|\psi^N_{\mathrm{in}}\right\rangle\right]$ with channel $\Lambda_{\omega;t}$ representing the overall single particle evolution over time t. To model the decoherence we consider the dephasing,

depolarization, loss and spontaneous emission maps, which corresponding Liouvillians can be found in Appendix A. As the estimated parameter corresponds now to $\omega = \varphi/t$, where φ is the phase of the unitary rotation, the QFI via a parameter change just rescales, so that $f_t[\varrho_\omega] = F_{\mathrm{Q}}[\varrho_\omega]\,/t = F_{\mathrm{Q}}[\varrho_\varphi]\,t$. Moreover, due to the commutativity of the unitary and the considered decoherence maps, we can without loss of generality utilize the results presented for them in the previous sections. Defining the channel QFI for frequency estimation tasks similarly to (7) as

$$\mathfrak{f}[\Lambda_\omega] = \max_{0\leq t\leq T} \max_{\psi_{\mathrm{in}}} f_t[\Lambda_{\omega;t}[|\psi_{\mathrm{in}}\rangle]] \tag{31}$$

we can compute all the appropriate expressions for QFIs and the asymptotic bounds of Table 1 as well as the finite-N bounds of (28) by substituting for the effective time dependence of the decoherence strength $\eta(t)$, which is determined by the master equation (30) (see Appendix A). Then, any quantity $\mathcal{F}$ listed in Table 1 transforms to its t-optimized equivalent as $\mathfrak{f} = \max_{0\leq t\leq T} \mathcal{F}\,t$. In Table 3 we present the channel QFIs relevant for frequency estimation, their asymptotic and finite-N CE bounds, as well as the maximal quantum precision enhancements for each model considered. In the case of dephasing, we recover the results of [24, 38, 40], whereas for depolarizing, loss and spontaneous emission maps we obtain the QFIs and their bounds, which to our knowledge have not been reported in the literature before. However, similarly to the case of quantum phase estimation summarized in Table 2, the obtained quantum enhancement factors for depolarization and spontaneous emission channels serve only as bounds, as they are not guaranteed to be saturable.

6. Estimation of decoherence strength

Lastly, we would like to emphasize that the CS, QS and CE methods described in Section 4 also apply to estimation tasks in which the estimated parameter is not encoded in the unitary, noiseless part of the system evolution. An example of such schemes are the experimentally motivated ones, in which one tries to quantify the effective strength of noise or loss present in the apparatus. That is why, we consider again the channels described in Appendix A, but this time with the parameter to be estimated being the decoherence strength η. This kind of problems has been widely considered not only in the estimation theory [44, 74–76], but also when examining issues of channel discrimination [45, 46] with particular application in quantum reading [50–52]. As compared to unitary rotations, the nature of the estimated parameter is dramatically different. In unitary parameter case, the use of entangled input state of N particles results in an effective N-times higher "angular speed" of rotation leading to the HL in the absence of noise. In decoherence strength estimation tasks, a change in the parameter value can be geometrically interpreted in the space of all valid quantum channels as a "movement" in the direction away from the boundary of the space of the relevant CPTP maps, which "speed" cannot be naively amplified N-times when employing N parallel channels. Hence, as in the case of lossy unitary rotation estimation, the optimal

Noise model	$\mathfrak{f}[\Lambda_\omega]$	$\mathfrak{f}[\Lambda_\omega\otimes\mathcal{I}]$	$\mathfrak{f}_N^{\mathrm{CE}}$ $(N\geq 2)$	$\mathfrak{f}_{\mathrm{as}}^{\mathrm{CE}}$	$\chi[\Lambda_\omega]$	$\chi[\Lambda_\omega\otimes\mathcal{I}]$
Dephasing	$\frac{1}{2\,\mathrm{e}\gamma}$	$\frac{1}{2\,\mathrm{e}\gamma}$	$\frac{N}{2\gamma}\frac{w_1[N]}{1+\left(\mathrm{e}^{w_1[N]}-1\right)N}$	$\frac{1}{2\gamma}$	$=\sqrt{\mathrm{e}}$	$=\sqrt{\mathrm{e}}$
Depolarization	$\frac{3}{4\,\mathrm{e}\gamma}$	$\approx 1.27\frac{3}{4\,\mathrm{e}\gamma}$	$\frac{3N}{4\gamma}\frac{\alpha\, w_\beta[N]}{2+\left(\mathrm{e}^{\frac{\alpha}{4}w_\beta[N]}-1\right)\left(\mathrm{e}^{\frac{\alpha}{4}w_\beta[N]}+2\right)N}$	$\frac{1}{\gamma}$	$\leq\sqrt{\frac{4\mathrm{e}}{3}}$	$\approx 0.89\sqrt{\frac{4\mathrm{e}}{3}}$
Loss	$\frac{1}{\mathrm{e}\gamma}$	$\frac{1}{\mathrm{e}\gamma}$	$\frac{N}{\gamma}\frac{w_1[N]}{1+\left(\mathrm{e}^{w_1[N]}-1\right)N}$	$\frac{1}{\gamma}$	$=\sqrt{\mathrm{e}}$	$=\sqrt{\mathrm{e}}$
Spontaneous emission	$\frac{1}{\mathrm{e}\gamma}$	$\frac{4\tilde{w}}{\gamma\left(1+\mathrm{e}^{\tilde{w}/2}\right)^2}$	$\frac{N}{\gamma}\frac{4\, w_4[N]}{4+\left(\mathrm{e}^{w_4[N]}-1\right)N}$	$\frac{4}{\gamma}$	$\leq\sqrt{2\mathrm{e}}$	$=\frac{1+\mathrm{e}^{\tilde{w}/2}}{\sqrt{\tilde{w}}}$

Table 3. QFIs, CE bounds and quantum enhancements in frequency estimation. In frequency estimation tasks the precision is maximized by adjusting the single experimental shot duration t. The t-optimised (extended) channel QFIs as well as their finite-N and asymptotic CE bounds are presented, where $w_x[N]=1+W\left[\frac{x-N}{\mathrm{e}N}\right]$, $\tilde{w}=1+2\,W\left[\frac{1}{2\sqrt{\mathrm{e}}}\right]$ and $W[x]$ is the Lambert W function. As in the case of depolarizing channel not all solutions possess an analytical form, only their numerical approximations are shown with $\alpha\approx 2.20$ and $\beta\approx 1.32$. Right of the double-line the maximal quantum precision enhancements are listed for the maps considered. In the case of dephasing noise the ultimate $\sqrt{\mathrm{e}}$ factor has already been reported in [24, 38]. For unextended depolarization and spontaneous emission maps, the derived enhancement factors may possibly be not achievable.

entangled inputs must lead not to scaling but constant factor quantum enhancements, which again can be quantified by the methods of Section 4. This also explains that for all the four noise models considered, the purely geometrical notion of classical simulability is enough to bound most tightly the maximal asymptotic precision of estimation. However, as for them also $\mathcal{F}_{\mathrm{as}}^{\mathrm{CS}}=\mathcal{F}_{\mathrm{as}}^{\mathrm{QS}}=\mathcal{F}_{\mathrm{as}}^{\mathrm{CE}}=\mathcal{F}\left[\Lambda_\eta\otimes\mathcal{I}\right]$, the CS-based asymptotic quantum enhancement corresponds to the classical estimation strategy that employs independent but extended channels. The fact that factorizable inputs — uncorrelated in between the extended N channels but possibly requiring entanglement between each single particle and its ancilla — are optimal for noise estimation with extended channels, has already been noticed for the low-noise [77] and generalized Pauli [78] channels, of which the latter contain the dephasing and depolarization maps here studied.

In the case of dephasing channel, we further realize that the extension at the single channel level is also unnecessary, as $\mathcal{F}\left[\Lambda_\eta\right]=\mathcal{F}\left[\Lambda_\eta\otimes\mathcal{I}\right]=1/(1-\eta^2)$, and the geometrically dictated bound of CS is attainable classically just by employing unentangled qubits in any pure state lying on the Bloch sphere equatorial plane. Similarly, the spontaneous emission and loss maps also turn out to be fully classical. In the first case, the asymptotic CS bound coincides with the extended and unextended channel QFIs derived in [79], whereas for the loss channel we obtain $\mathcal{F}_{\mathrm{as}}^{\mathrm{CS}}=\mathcal{F}\left[\Lambda_\eta\right]=\mathcal{F}\left[\Lambda_\eta\otimes\mathcal{I}\right]=1/(\eta(1-\eta))$, which at the single channel level is achieved by a photon in any mixed state with the ancilla being redundant. On the one hand, this emphasizes that entanglement between the photons entering the interferometer is unnecessary and

Channel considered	$\mathcal{F}[\Lambda_\eta]$	$\mathcal{F}[\Lambda_\eta \otimes \mathcal{I}]$	$\mathcal{F}_{\rm as}^{\rm CS} = \mathcal{F}_{\rm as}^{\rm QS} = \mathcal{F}_{\rm as}^{\rm CE}$
Dephasing	$\frac{1}{1-\eta^2}$	$\frac{1}{1-\eta^2}$	$\frac{1}{1-\eta^2}$ [78]
Depolarization	$\frac{1}{1-\eta^2}$ [69]	$\frac{3}{(1-\eta)(1+3\eta)}$ [69]	$\frac{3}{(1-\eta)(1+3\eta)}$ [35, 78]
Loss	$\frac{1}{\eta(1-\eta)}$	$\frac{1}{\eta(1-\eta)}$	$\frac{1}{\eta(1-\eta)}$
Spontaneous emission	$\frac{1}{\eta(1-\eta)}$ [79]	$\frac{1}{\eta(1-\eta)}$ [79]	$\frac{1}{\eta(1-\eta)}$

Table 4. Decoherence strength estimation quantified via channel QFIs and their asymptotic bounds. Definitions of channels listed in the first column can be found in Appendix A. In contrast to phase estimation examples given in Table 1, the variable to be estimated here is the decoherence parameter η, $(0 \leq \eta < 1)$. Due to the different nature of the estimated parameter, the geometrical classical simulation (CS) method provides bounds that not just most tightly limit the asymptotic extended channel QFIs, but actually coincide with its value. The results prove that only in the case of depolarization channel the precision can be enhanced with the use of quantum estimation strategies, as for all other cases $\mathcal{F}[\Lambda_\eta] = \mathcal{F}[\Lambda_\eta \otimes \mathcal{I}] = \mathcal{F}_{\rm as}$.

agrees with the results of [74, 75] confirming that the total photon number fluctuations are really the ones that limit the precision. These can be reduced by employing Gaussian states [74] or in principle fully eliminated by the use of Fock states [75] that attain the CS-bound.

The case of depolarization map is different, as it is known that for qubits [69, 80] the precision of estimation may be improved by extending the channel, i.e. $\mathcal{F}[\Lambda_\eta] < \mathcal{F}[\Lambda_\eta \otimes \mathcal{I}]$. This leaves the space for possible enhancement thanks to the use of entangled probes *between unextended* channels and indeed this fact has been observed already when considering two depolarization channels used in parallel [69]. The results are summarized in Table 4.

7. Summary

We would also like to point that the SQL-like bounds, universally valid in practical metrological scenarios, allow to avoid some of the controversies characteristic for idealized decoherence-free scenarios. When decoherence is *not* present and the probe states with indefinite number of particles are considered, such as e.g. squeezed states of light, the exact form of HL needs to be reconsidered [81–83] since the direct replacement of N with mean number of particles $\bar{N}$ may make the HL invalid. Moreover, the final claims on the achievable precision scaling may strongly depend on the form of a priori parameter knowledge assumed, and lead to some apparent contradictions [84, 85]. These difficulties do not arise in the realistic metrological schemes, as the asymptotic SQL-like bounds are valid also when N is replaced by $\bar{N}$ for indefinite particle number

state [39, 86]. The bounds derived in the so-called *local approach* (small parameter fluctuation) based on the calculation of the *Quantum Fisher Information* (QFI) are saturable in a single-shot scenario unlike the decoherence-free case when only after some number of independently repeated experiments one may expect to approach the theoretical limits [87]. This is due to the fact that by employing input states of grouped particles, which possess no correlations in between the groupings, and by letting the groups to be of finite but sufficiently large size, one can attain the ultimate asymptotic SQL bound up to any precision. Since saturability of the quantum Fisher information bounds for independently prepared probes is well established [61–63, 88], the operational meaning of the QFI is clear also in the single shot scenario.

We also conjecture from the point of view of the asymptotic SQL-like bounds that the specific form of the a priori knowledge should not play an important role. In particular, we expect that various methods such as *Bayesian* [89–92] or *information theoretic* [93, 94] should recover the bounds compatible with the ones obtained via the *local approach* considered in this paper. This statement is known to hold in the case of optical interferometry with losses [31, 32] and it is an intriguing question whether analogous claims can be made in more general scenarios.

Acknowledgments

We would like to thank Konrad Banaszek for constant support and Mădălin Guţă for valuable feedback. J.K. acknowledges Michal Sedlák and Jonatan Bohr Brask for helpful comments and thanks Marcin Jarzyna for many fruitful discussions as well as the data utilized in Figure 3. This research was supported by Polish NCBiR under the ERA-NET CHIST-ERA project QUASAR, Foundation for Polish Science TEAM project co-financed by the EU European Regional Development Fund and FP7 IP project Q-ESSENCE.

Appendix A. Channels considered

We adopt the standard notation in which $\mathbb{I}_d$ represents a $d\times d$ identity matrix and $\{\sigma_i\}_{i=1}^3$ are the Pauli operators. In Section 4.2 parameter φ to be estimated is the rotation angle around the z axis of the Bloch ball generated by the unitary operator $U_\varphi = \exp[\mathrm{i}\sigma_3\varphi/2]$. We consider maps $\mathcal{D}_\eta$ with decoherence parameter η that commute with such rotation, whence $\Lambda_\varphi[\varrho] = \mathcal{D}_\eta\big[U_\varphi \varrho U_\varphi^\dagger\big] = U_\varphi \mathcal{D}_\eta[\varrho]\, U_\varphi^\dagger$, and are defined accordingly by the Kraus operators presented below. For each case, we also specify the purification determining the extended channel QFI (12) ($\mathcal{F}[\Lambda_\varphi \otimes \mathcal{I}]$ in Table 1) in the form of the optimal generator of Kraus representation rotation h, as introduced in (10). Dealing with frequency estimation tasks discussed in Section 5 we construct the effective one-particle Kraus operators by substituting $\varphi \to \omega t$ and $\eta \to \eta(t)$ in the nominal ones, where ω is the estimated frequency detuning. For all models, we explicitly write the Liouvillian $\mathcal{L}^{(n)}$ determining the noise affecting each particle, see (30), and the effective form of $\eta(t)$.

When discussing decoherence strength estimation in Section 6, we consider solely each of the following noise maps with η being now the parameter to be estimated: $\Lambda_{\varphi=\eta}=\mathcal{D}_\eta$.

Appendix A.1. Dephasing

- *Decoherence parameter*, η, represents the final equatorial radius of the Bloch ball shrank uniformly in the xy plane by the channel.
- *Kraus operators*:

$$K_1=\sqrt{\frac{1+\eta}{2}}\,\mathbb{I}_2\,,\quad K_2=\sqrt{\frac{1-\eta}{2}}\,\sigma_3\,. \tag{A.1}$$

- *Optimal purification* determining the extended channel QFI (12):

$$h=\frac{\sqrt{1-\eta^2}}{2}\,\sigma_1\,. \tag{A.2}$$

- *One-particle Liouvillian* for frequency estimation tasks:

$$\mathcal{L}^{(n)}[\varrho]=\frac{\gamma}{2}\left(\sigma_3^{(n)}\varrho\,\sigma_3^{(n)}-\varrho\right)\qquad\therefore\quad\eta(t)=\mathrm{e}^{-\gamma t}. \tag{A.3}$$

Appendix A.2. Depolarization

- *Decoherence parameter*, η, represents the final radius of the Bloch ball shrank isotropically by the channel.
- *Kraus operators*:

$$K_1=\sqrt{\frac{1+3\eta}{4}}\,\mathbb{I}_2\,,\quad\left\{K_i=\sqrt{\frac{1-\eta}{4}}\,\sigma_{i-1}\right\}_{i=2\ldots4}. \tag{A.4}$$

- *Optimal purification* determining the extended channel QFI (12):

$$h=\frac{1}{2}\begin{pmatrix}0&0&0&\xi\\0&\multicolumn{2}{c}{\multirow{2}{*}{σ_2}}&0\\0&&&0\\\xi&0&0&0\end{pmatrix}\quad\text{with}\quad\xi=\frac{\sqrt{(1+3\eta)\,(1-\eta)}}{1+\eta}. \tag{A.5}$$

- *One-particle Liouvillian* for frequency estimation tasks:

$$\mathcal{L}^{(n)}[\varrho]=\frac{\gamma}{2}\left(\frac{1}{3}\sum_{i=1}^{3}\sigma_i^{(n)}\varrho\,\sigma_i^{(n)}-\varrho\right)\qquad\therefore\quad\eta(t)=\mathrm{e}^{-\frac{2\gamma}{3}t}. \tag{A.6}$$

Appendix A.3. Loss

- *Decoherence parameter*, η, represents survival probability of each of the particles that are subject to independent loss processes. The channel on a single particle is formally a map from a two- to a three-dimensional system with output's third dimension corresponding to the vacuum mode responsible for the particle loss. Although, in this case one should strictly write $\Lambda_\varphi=\mathcal{D}_\eta\left[U_\varphi\varrho U_\varphi^\dagger\right]=\tilde{U}_\varphi\,\mathcal{D}_\eta[\varrho]\,\tilde{U}_\varphi^\dagger$ with $\tilde{U}_\varphi$ acting on a different Hilbert space, the effects of U_φ and $\tilde{U}_\varphi$ are physically

indistinguishable, as the particle losses commute with the acquired phase (for instance see [30]).

- *Kraus operators*:

$$K_1 = \begin{pmatrix} 0 & 0 \\ 0 & 0 \\ 0 & \sqrt{1-\eta} \end{pmatrix},\ K_2 = \begin{pmatrix} 0 & 0 \\ 0 & 0 \\ \sqrt{1-\eta} & 0 \end{pmatrix},\ K_3 = \begin{pmatrix} \sqrt{\eta} & 0 \\ 0 & \sqrt{\eta} \\ 0 & 0 \end{pmatrix}. \tag{A.7}$$

- *Optimal purification* determining the extended channel QFI (12):

$$h = -\frac{1}{2}\begin{pmatrix} \begin{bmatrix} \sigma_3 \end{bmatrix} & 0 \\ 0\ \ 0 & 0 \end{pmatrix}. \tag{A.8}$$

- *One-particle Liouvillian* for the frequency estimation tasks:

$$\mathcal{L}^{(n)}[\varrho] = \gamma \sum_{m=0}^{1} \left(\sigma_{m,+}^{(n)} \varrho\, \sigma_{m,-}^{(n)} - \frac{1}{2}\left\{ \sigma_{m,-}^{(n)} \sigma_{m,+}^{(n)}, \varrho \right\} \right) \qquad \therefore \quad \eta(t) = \mathrm{e}^{-\gamma t}, \tag{A.9}$$

where $\sigma_{m,+}^{(n)} = |\mathrm{vac}\rangle\langle m|$ are the generators of transition to the vacuum mode from qubit basis states $|0\rangle$ and $|1\rangle$, such that $\sigma_{m,-}^{(n)} = \sigma_{m,+}^{(n)\dagger}$.

Appendix A.4. Spontaneous emission (amplitude damping)

- *Decoherence parameter*, η, represents the radius of the disk obtained by projecting the deformed Bloch ball outputted by the channel onto the xy plane.
- *Kraus operators*:

$$K_1 = \begin{pmatrix} 1 & 0 \\ 0 & \sqrt{\eta} \end{pmatrix}, \quad K_2 = \begin{pmatrix} 0 & \sqrt{1-\eta} \\ 0 & 0 \end{pmatrix}. \tag{A.10}$$

- *Optimal purification* determining the extended channel QFI (12):

$$h = \frac{1}{2}\begin{pmatrix} \xi & 0 \\ 0 & -1 \end{pmatrix} \quad \text{with} \quad \xi = \frac{1-\sqrt{\eta}}{1+\sqrt{\eta}}. \tag{A.11}$$

- *One-particle Liouvillian* for the frequency estimation tasks ($\sigma_\pm = \frac{1}{2}(\sigma_1 \pm \mathrm{i}\sigma_2)$):

$$\mathcal{L}^{(n)}[\varrho] = \gamma \left(\sigma_{+}^{(n)} \varrho\, \sigma_{-}^{(n)} - \frac{1}{2}\left\{ \sigma_{-}^{(n)} \sigma_{+}^{(n)}, \varrho \right\} \right) \qquad \therefore \quad \eta(t) = \mathrm{e}^{-\gamma t}. \tag{A.12}$$

Appendix B. Equivalence of RLD-based bound applicability and local classical simulability of a channel

Given a channel — a CPTP map $\Lambda_\varphi : \mathcal{H}_{\mathrm{in}} \to \mathcal{H}_{\mathrm{out}}$ — we define its Choi-Jamiolkowski (C-J) matrix representation [60] as $\Omega_{\Lambda_\varphi} = \Lambda_\varphi \otimes \mathcal{I}\,[|\mathbb{I}\rangle\langle\mathbb{I}|] = \sum_i |K_i(\varphi)\rangle\langle K_i(\varphi)|$, where $\{K_i(\varphi)\}_{i=1}^r$ are r linearly independent Kraus operators of Λ_φ, and adopt a concise notation for bipartite states, in which $|\phi\rangle = \sum_{i,j=1}^{\dim \mathcal{H}_{in}} \langle i|\phi|j\rangle\, |i\rangle\, |j\rangle = \phi \otimes \mathbb{I}\, |\mathbb{I}\rangle = \mathbb{I} \otimes \phi^T\, |\mathbb{I}\rangle$ with $|\mathbb{I}\rangle = \sum_{i=1}^{\dim \mathcal{H}_{in}} |i\rangle\, |i\rangle$. For simplicity, from now onwards we drop the explicit φ

dependence of operators, assuming that the estimation is performed for small variations $\delta\varphi$ around a given, fixed φ. In Sup. Mat. of [39] (Equation (S9)) it has been proven that the condition for any channel to be φ-non-extremal (classically simulable) at φ is equivalent to the statement that there exists a non-zero Hermitian matrix μ_{ij} such that

$$\dot{\Omega}_{\Lambda_\varphi} = \sum_{ij} \mu_{ij} \, |K_i\rangle\langle K_j|. \tag{B.1}$$

On the other hand, the RLD-based bound exists there if and only if [37]

$$P_{\Omega_\perp} \dot{\Omega}^2_{\Lambda_\varphi} P_{\Omega_\perp} = 0 \tag{B.2}$$

where $P_{\Omega_\perp}$ is the projection onto the null-space $\Omega_\perp$, i.e. the subspace orthogonal to Ω_{Λ_φ}, so that $\forall_i\colon\ P_{\Omega_\perp} \, |K_i\rangle = 0$. The (B.1) implies (B.2), as by substitution

$$P_{\Omega_\perp} \left(\sum_{ij} \mu_{ij} \, |K_i\rangle\langle K_j| \right)^2 P_{\Omega_\perp} = \sum_{ij} \left(\sum_{p} \mu_{ip} \, \langle K_p|K_p\rangle \, \mu_{pj} \right) P_{\Omega_\perp} \, |K_i\rangle\langle K_j| \, P_{\Omega_\perp} = 0 \,, \tag{B.3}$$

thus any φ-non-extremal channel must admit an RLD-based bound on its extended QFI. In order to prove the other direction, we split the derivatives of each C-J eigenvector into components supported by Ω_{Λ_φ} and in the null-space $\Omega_\perp$: $\left|\dot{K}_i\right\rangle = \sum_j \nu_{ij} \, |K_j\rangle + \left|K_i^\perp\right\rangle$. Hence, after substituting for $\dot{\Omega}_{\Lambda_\varphi}$ the (B.2) then simplifies to

$$\left(\sum_i \left|K_i^\perp\right\rangle\langle K_i| \right) \left(\sum_j |K_j\rangle\left\langle K_j^\perp\right| \right) = 0, \tag{B.4}$$

and since $A^\dagger A = 0$ implies $A^\dagger = A = 0$ and $\{|K_i\rangle\}_i$ are orthogonal, we conclude that all $\left|K_i^\perp\right\rangle = 0$. Thus, (B.2) implies that $\left|\dot{K}_i\right\rangle = \sum_j \nu_{ij} \, |K_j\rangle$, which due to the local ambiguity of Kraus representations (9) is equivalent to $\left|\dot{\tilde{K}}_i\right\rangle = \sum_j (\nu_{ij} - \mathrm{i}\, h_{ij}) \left|\tilde{K}_j\right\rangle$ for any Hermitian h. Therefore, without loss of generality, we may set $h = -\frac{\mathrm{i}}{2}\nu^{\mathrm{AH}}$ after splitting ν into its Hermitian and anti-Hermitian parts $\nu = \nu^{\mathrm{H}} + \nu^{\mathrm{AH}}$, so that $\left|\dot{\tilde{K}}_i\right\rangle = \sum_j \nu^{\mathrm{H}}_{ij} \left|\tilde{K}_j\right\rangle$ with $\nu^{\mathrm{H}} \neq 0$ for any non-trivial channel. Finally, we can write

$$\dot{\Omega}_\varphi = \sum_i \left|\dot{\tilde{K}}_i\right\rangle\left\langle \tilde{K}_i\right| + \left|\tilde{K}_i\right\rangle\left\langle \dot{\tilde{K}}_i\right| = 2 \sum_{ij} \nu^{\mathrm{H}}_{ji} \left|\tilde{K}_i\right\rangle\left\langle \tilde{K}_j\right| \tag{B.5}$$

and satisfy the condition (B.1).■

Appendix C. RLD-based bound as a special case of asymptotic CE bound

For a channel that admits an RLD-based bound, in order to obtain the CS condition (B.5) in Appendix B, we chose $h = -\frac{\mathrm{i}}{2}\nu^{\mathrm{AH}}$ that actually satisfies the $\beta_{\tilde{K}} = 0$ constraint (24) of the CE method. This can be verified by taking the $\mathrm{Tr}_{\mathcal{H}_{\mathrm{out}}}\{\ldots\}$ of the both sides of the identity

$$\sum_{ij} h_{ij} \, |K_j\rangle\langle K_i| = \sum_{ij} \frac{\mathrm{i}}{2} \left(\nu_{ij} - \nu_{ij}^\dagger \right) |K_j\rangle\langle K_i| = \frac{\mathrm{i}}{2} \sum_i \left|\dot{K}_i\right\rangle\langle K_i| - |K_i\rangle\left\langle \dot{K}_i\right|, \tag{C.1}$$

which results in (24). This is consistent, as the CE method must apply to any φ-non-extremal channel [39] — admitting an RLD-based bound. Furthermore, the asymptotic CE bound (25) is at least as tight as the RLD-based bound (13) on the extended channel QFI (12). We prove this by substituting (B.5) into the definition of $\mathcal{F}^{\mathrm{RLD}}[\Lambda_\varphi \otimes \mathcal{I}]$ in (13), so that

$$\mathcal{F}^{\mathrm{RLD}}[\Lambda_\varphi \otimes \mathcal{I}] = 4 \left\| \mathrm{Tr}_{\mathcal{H}_{\mathrm{out}}} \left\{ \sum_{ij} \nu^{\mathrm{H}}_{ji} \left| \tilde{K}_i \right\rangle \sum_{pq} \nu^{\mathrm{H}}_{pq} \left\langle \tilde{K}_q \right| \right\} \right\| = 4 \left\| \sum_i \dot{\tilde{K}}_i^\dagger \dot{\tilde{K}}_i \right\|, \quad \text{(C.2)}$$

where we have used the fact that $\left\langle \tilde{K}_j \right| \Omega_\varphi^{-1} \left| \tilde{K}_p \right\rangle = \delta_{jp}$. Hence, $\mathcal{F}^{\mathrm{RLD}}[\Lambda_\varphi \otimes \mathcal{I}]$ is an example of an asymptotic CE-based bound with a possibly sub-optimal Kraus representation chosen such that $\forall_i : \left| \dot{\tilde{K}}_i \right\rangle = \sum_j \nu^{\mathrm{H}}_{ij} \left| \tilde{K}_j \right\rangle$ and $\beta_{\tilde{K}} = 0$.■

Appendix D. Optimal local QS of a channel

A channel Λ_φ of rank r, in order to be locally quantum simulable within small deviations $\delta\varphi$ from a given φ, must fulfil the condition (see Section 4.1.2)

$$\Lambda_\varphi[\varrho] = \mathrm{Tr}_{\mathrm{E}_\Phi \mathrm{E}_\sigma} \left\{ U \left(\varrho \otimes |\psi_\varphi\rangle\langle\psi_\varphi| \right) U^\dagger \right\} + O(\delta\varphi^2) = \sum_{i=1}^{r' \geq r} \bar{K}_i(\varphi)\, \varrho\, \bar{K}_i(\varphi)^\dagger + O(\delta\varphi^2), \quad \text{(D.1)}$$

where $\bar{K}_i(\varphi) = \langle i| U |\psi_\varphi\rangle$ and $\{|i\rangle\}_{i=1}^{r'}$ form any basis in the r' dimensional $\mathcal{H}_{\mathrm{E}_\Phi} \times \mathcal{H}_{\mathrm{E}_\sigma}$ space containing ψ_φ. Hence, Λ_φ must admit a Kraus representation $\{\tilde{K}_i\}_{i=1}^{r'}$ (with possibly linearly dependent Kraus operators, as for generality we assume $r' \geq r$) that coincides with the one of (D.1) up to $O(\delta\varphi^2)$, i.e. satisfies $\tilde{K}_i = \bar{K}_i$ and $\dot{\tilde{K}}_i = \dot{\bar{K}}_i$ for all i. We construct a valid decomposition of $|\dot{\psi}_\varphi\rangle$ into its (normalized) components parallel and perpendicular to ψ_φ: $\left|\dot{\psi}_\varphi\right\rangle = \mathrm{i}\, a |\psi_\varphi\rangle - \mathrm{i}\, b \left|\psi_\varphi^\perp\right\rangle$, where we can choose $a, b \in \mathbb{R}$ because of $\partial_\varphi \langle\psi_\varphi|\psi_\varphi\rangle = 0$ and the irrelevance of the global phase. Then, the asymptotic bound $\mathcal{F}^{\mathrm{bound}}_{\mathrm{as}}$ of (18) determined by the local QS (D.1) at φ simply reads $F_{\mathrm{Q}}[|\psi_\varphi\rangle] = 4b^2$ and the required Kraus operators $\{\tilde{K}_i\}_{i=1}^{r'}$ of Λ_φ must fulfil conditions $\tilde{K}_i = \langle i| U |\psi_\varphi\rangle$ and $\dot{\tilde{K}}_i = \langle i| U \left|\dot{\psi}_\varphi\right\rangle = \mathrm{i}\, a \tilde{K}_i - \mathrm{i}\, b \langle i| U \left|\psi_\varphi^\perp\right\rangle$. Hence, for the local QS of channel Λ_φ to be valid, we must be able always to construct

$$U = \begin{bmatrix} \tilde{K}_1 & \frac{a}{b}\tilde{K}_1 + \frac{\mathrm{i}}{b}\dot{\tilde{K}}_1 & \bullet & \dots & \bullet \\ \tilde{K}_2 & \frac{a}{b}\tilde{K}_2 + \frac{\mathrm{i}}{b}\dot{\tilde{K}}_2 & \bullet & \dots & \bullet \\ \tilde{K}_3 & \frac{a}{b}\tilde{K}_3 + \frac{\mathrm{i}}{b}\dot{\tilde{K}}_3 & \vdots & \ddots & \vdots \\ \vdots & \vdots & \bullet & \dots & \bullet \end{bmatrix} \quad \text{(D.2)}$$

with first two columns fixed to give for all i the correct $\langle i| U |\psi_\varphi\rangle$ and $\langle i| U \left|\psi_\varphi^\perp\right\rangle$ respectively. Due to locality, all entries marked with $\bullet$ in (D.2) can be chosen freely to satisfy the unitarity condition $U^\dagger U = U U^\dagger = \mathbb{I}$. Yet, this constraint still requires the Kraus operators to simultaneously fulfil $\mathrm{i} \sum_{i=1}^{r'} \dot{\tilde{K}}_i^\dagger \tilde{K}_i = a\, \mathbb{I}$ and $\sum_{i=1}^{r'} \dot{\tilde{K}}_i^\dagger \dot{\tilde{K}}_i = (b^2 + a^2)\, \mathbb{I}$. Without loss of generality, we may shift their phase at φ, so that $\tilde{K}_i \to \mathrm{e}^{-\mathrm{i}a\varphi} \tilde{K}_i$ and

the conditions become independent of a, i.e. $\mathrm{i}\sum_{i=1}^{r'}\dot{\tilde{K}}_i^\dagger\tilde{K}_i = 0$ and $\sum_{i=1}^{r'}\dot{\tilde{K}}_i^\dagger\dot{\tilde{K}}_i = b^2\mathbb{I}$. Furthermore, these constraints do not require $r'>r$, as rewriting for example the first one as $\mathrm{i}\sum_{i=1}^{r'}\left\langle\dot{\psi}_\varphi\right| U\left|i\right\rangle\left\langle i\right| U\left|\psi_\varphi\right\rangle = 0$, one can always resolve the identity with some basis vectors $\sum_{i=1}^{r'}|i\rangle\langle i| = \sum_{i=1}^{r}|e_i\rangle\langle e_i|$ and define linear independent Kraus operators $\{K_i = \langle e_i| U|\psi_\varphi\rangle\}_{i=1}^{r}$ also fulfilling the necessary requirements.

Finally, we may conclude that Λ_φ is locally *quantum simulable* at φ, if it admits there a Kraus representation satisfying conditions (21) stated in the main text, which due to locality can be generated via (9) by some Hermitian $r\times r$ matrix h.■

Appendix E. Finite-N CE method as a semi-definite programming task

The finite-N CE bound has been defined in (27) as

$$\mathcal{F}_N^{\mathrm{CE}} = 4\min_h\left\{\|\alpha_{\tilde{K}}\| + (N-1)\,\|\beta_{\tilde{K}}\|^2\right\}, \tag{E.1}$$

where $\|\cdot\|$ denotes the operator norm, $\alpha_{\tilde{K}} = \sum_i \dot{\tilde{K}}_i^\dagger\dot{\tilde{K}}_i$ and $\beta_{\tilde{K}} = \mathrm{i}\sum_i \dot{\tilde{K}}_i^\dagger\tilde{K}_i$. Given a channel Λ_φ from a d_{in}- to a d_{out}-dimensional Hilbert space and the set of its linearly independent Kraus operators ($d_{\mathrm{out}}\times d_{\mathrm{in}}$ matrices) $\{K_i\}_{i=1}^r$, in order to compute $\mathcal{F}_N^{\mathrm{CE}}$, we should minimize (E.1) over locally equivalent Kraus representations (9) of Λ_φ generated by all Hermitian, $r\times r$ matrices h.

Basing on the results of [39], where the $\beta_{\tilde{K}}=0$ constraint (24) is also imposed on (E.1), we show that $\mathcal{F}_N^{\mathrm{CE}}$ can always be evaluated by means of semi-definite programming (SDP). Adopting a concise notation in which $\mathbf{K}$ is a column vector containing the starting Kraus operators K_i as its elements, we can associate all locally equivalent Kraus representations $\tilde{\mathbf{K}}$ in (E.1) with those generated by any h via $\tilde{\mathbf{K}}=\mathbf{K}$ and $\dot{\tilde{\mathbf{K}}}=\dot{\mathbf{K}}-\mathrm{i}h\mathbf{K}$. By constructing matrices ($\mathbb{I}_d$ represents a $d\times d$ identity matrix)

$$\mathbf{A} = \begin{bmatrix} \sqrt{\lambda_a}\mathbb{I}_{d_{\mathrm{in}}} & \dot{\tilde{\mathbf{K}}}^\dagger \\ \dot{\tilde{\mathbf{K}}} & \sqrt{\lambda_a}\mathbb{I}_{r\cdot d_{\mathrm{out}}} \end{bmatrix} \qquad \mathbf{B} = \begin{bmatrix} \sqrt{\lambda_b}\mathbb{I}_{d_{\mathrm{in}}} & \left(\mathrm{i}\dot{\tilde{\mathbf{K}}}^\dagger\tilde{\mathbf{K}}\right)^\dagger \\ \mathrm{i}\dot{\tilde{\mathbf{K}}}^\dagger\tilde{\mathbf{K}} & \sqrt{\lambda_b}\mathbb{I}_{d_{\mathrm{in}}} \end{bmatrix}, \tag{E.2}$$

which positive semi-definiteness conditions correspond respectively to

$$\alpha_{\tilde{K}} = \dot{\tilde{\mathbf{K}}}^\dagger\dot{\tilde{\mathbf{K}}} \;\leq\; \lambda_a\mathbb{I}_{d_{\mathrm{in}}} \qquad \beta_{\tilde{K}}^\dagger\beta_{\tilde{K}} = \tilde{\mathbf{K}}^\dagger\dot{\tilde{\mathbf{K}}}\dot{\tilde{\mathbf{K}}}^\dagger\tilde{\mathbf{K}} \;\leq\; \lambda_b\mathbb{I}_{d_{\mathrm{in}}}, \tag{E.3}$$

we rewrite (E.1) into the required SDP form

$$\begin{aligned}\mathcal{F}_N^{\mathrm{CE}} &= 4\min_h\left\{\lambda_a + (N-1)\lambda_b\right\}, \\ &\text{subject to: } \mathbf{A}\geq 0,\ \mathbf{B}\geq 0.\end{aligned} \tag{E.4}$$

For the purpose of this paper we have implemented a semi-definite program using the CVX package for Matlab [95], which efficiently evaluates (E.4) given the set of Kraus operators and their derivatives of a generic channel Λ_φ. The fact that only $\mathbf{K}$ and $\dot{\mathbf{K}}$ are involved in (E.4) is a consequence of the QFI, and hence the bound $\mathcal{F}_N^{\mathrm{CE}}$, being a local quantity.

Lastly, one should note that by slightly modifying the program in (E.4) we are able to also efficiently evaluate: the extended channel QFI (12), as $\mathcal{F}[\Lambda_\varphi \otimes \mathcal{I}] = \mathcal{F}^{\rm CE}_{N=1}$; and the asymptotic extended channel QFI (25), $\mathcal{F}_{\rm as}[\Lambda_\varphi \otimes \mathcal{I}] = \mathcal{F}^{\rm CE}_{\rm as}$, by setting $N = 1$ and imposing the $\beta_{\tilde{K}} = 0$ constraint (24) as already pursued in [39].

References

[1] Leibfried D, Barrett M D, Schaetz T, Britton J, Chiaverini J, Itano W M, Jost J D, Langer C and Wineland D J 2004 *Science* **304** 1476–1478

[2] Schmidt P O, Rosenband T, Langer C, Itano W M, Bergquist J C and Wineland D J 2005 *Science* **309** 749–752

[3] Roos C F, Chwalla M, Kim K, Riebe M and Blatt R 2006 *Nature* **443** 316–319 ISSN 0028-0836

[4] Ospelkaus C, Warring U, Colombe Y, Brown K R, Amini J M, Leibfried D and Wineland D J 2011 *Nature* **476** 181–184

[5] Wasilewski W, Jensen K, Krauter H, Renema J J, Balabas M V and Polzik E S 2010 *Phys. Rev. Lett.* **104** 133601

[6] Wolfgramm F, Cerè A, Beduini F A, Predojević A, Koschorreck M and Mitchell M W 2010 *Phys. Rev. Lett.* **105** 053601

[7] Koschorreck M, Napolitano M, Dubost B and Mitchell M W 2010 *Phys. Rev. Lett.* **104** 093602

[8] Mitchell M W, Lundeen J S and Steinberg A M 2004 *Nature* **429** 161–164

[9] Nagata T, Okamoto R, O'Brien J L, Sasaki K and Takeuchi S 2007 *Science* **316** 726–729

[10] Resch K J, Pregnell K L, Prevedel R, Gilchrist A, Pryde G J, O'Brien J L and White A G 2007 *Phys. Rev. Lett.* **98** 223601

[11] Higgins B L, Berry D W, Bartlett S D, Mitchell M W, Wiseman H M and Pryde G J 2009 *New J. Phys.* **11** 073023

[12] LIGO Collaboration 2011 *Nature Phys.* **7** 962–965

[13] D J Wineland J J Bollinger W M I and Moore F L 1992 *Phys. Rev. A* **46** R6797–R6800

[14] Bollinger J J, Itano W M, Wineland D J and Heinzen D J 1996 *Phys. Rev. A* **54** R4649–R4652

[15] Bužek V, Derka R and Massar S 1999 *Phys. Rev. Lett.* **82** 2207–2210

[16] Berry D W and Wiseman H M 2000 *Phys. Rev. Lett.* **85** 5098–5101

[17] Giovannetti V, Lloyd S and Maccone L 2006 *Phys. Rev. Lett.* **96** 010401

[18] Banaszek K, Demkowicz-Dobrzanski R and Walmsley I A 2009 *Nature Photon.* **3** 673–676

[19] Giovannetti V, Lloyd S and Maccone L 2011 *Nature Photon.* **5** 222–229

[20] Maccone L and Giovannetti V 2011 *Nature Phys.* **7** 376–377

[21] Dowling J P 2008 *Contemp. Phys.* **49** 125–143

[22] Andrè A, Sørensen A S and Lukin M D 2004 *Phys. Rev. Lett.* **92** 230801

[23] Auzinsh M, Budker D, Kimball D F and Rochester S M 2004 *Phys. Rev. Lett.* **93** 173002

[24] Huelga S F, Macchiavello C, Pellizzari T, Ekert A K, Plenio M B and Cirac J I 1997 *Phys. Rev. Lett.* **79** 3865–3868

[25] Shaji A and Caves C M 2007 *Phys. Rev. A* **76** 032111

[26] Dorner U 2012 *New J. Phys.* **14** 043011

[27] Huver S D, Wildfeuer C F and Dowling J P 2008 *Phys. Rev. A* **78** 063828

[28] Meiser D and Holland M J 2009 *New J. Phys.* **11** 033002

[29] Dorner U, Demkowicz-Dobrzański R, Smith B J, Lundeen J S, Wasilewski W, Banaszek K and Walmsley I A 2009 *Phys. Rev. Lett.* **102** 040403

[30] Demkowicz-Dobrzański R, Dorner U, Smith B, Lundeen J S, Wasilewski W, Banaszek K and Walmsley I A 2009 *Phys. Rev. A* **80** 013825

[31] Kołodyński J and Demkowicz-Dobrzański R 2010 *Phys. Rev. A* **82** 053804

[32] Knysh S, Smelyanskiy V N and Durkin G A 2011 *Phys. Rev. A* **83** 021804

[33] Sarovar M and Milburn G J 2006 *J. Phys. A: Math. Gen.* **39** 8487

[34] Ji Z, Wang G, Duan R, Feng Y and Ying M 2008 *IEEE Trans. Inf. Theory* **54** 5172 –5185

[35] Fujiwara A and Imai H 2008 *J. Phys. A: Math. Theor.* **41** 255304

[36] Matsumoto K 2010 *ArXiv e-prints* 1006.0300

[37] Hayashi M 2011 *Comm. Math. Phys.* **304** 689–709

[38] Escher B M, de Matos Filho R L and Davidovich L 2011 *Nature Phys.* **7** 406–411

[39] Demkowicz-Dobrzański R, Kołodyński J and Guţă M 2012 *Nat. Commun.* **3** 1063

[40] Chaves R, Brask J B, Markiewicz M, Kołodyński J and Acin A 2012 *ArXiv e-prints* 1212.3286

[41] Acín A, Jané E and Vidal G 2001 *Phys. Rev. A* **64** 050302(R)

[42] D'Ariano G M, Presti P L and Paris M G A 2001 *Phys. Rev. Lett.* **87** 270404

[43] Chiribella G, D'Ariano G M, Perinotti P and Sacchi M F 2004 *Phys. Rev. Lett.* **93** 180503

[44] Hotta M, Karasawa T and Ozawa M 2005 *Phys. Rev. A* **72** 052334

[45] Sacchi M F 2005 *Phys. Rev. A* **71** 062340

[46] D'Ariano G M, Sacchi M F and Kahn J 2005 *Phys. Rev. A* **72** 052302

[47] Chiribella G, D'Ariano G M and Perinotti P 2008 *Phys. Rev. Lett.* **101** 180501

[48] Sedlák M and Ziman M 2009 *Phys. Rev. A* **79** 012303

[49] Bisio A, D'Ariano G M, Perinotti P and Sedlák M 2012 *Phys. Rev. A* **85** 032333

[50] Pirandola S 2011 *Phys. Rev. Lett.* **106** 090504

[51] Pirandola S, Lupo C, Giovannetti V, Mancini S and Braunstein S L 2011 *New J. Phys.* **13** 113012

[52] Nair R 2011 *Phys. Rev. A* **84** 032312

[53] Nair R and Yen B J 2011 *Phys. Rev. Lett.* **107** 193602

[54] Breuer H P and Petruccione F 2002 *The Theory of Open Quantum Systems* (Oxford University Press)

[55] Andersson E, Cresser J D and Hall M J W 2007 *J. Mod. Opt.* **54** 1695

[56] Chin A W, Huelga S F and Plenio M B 2012 *Phys. Rev. Lett.* **109** 233601

[57] Szankowski P, Chwedenczuk J and Trippenbach M 2012 *ArXiv e-prints* 1212.2528

[58] Kay S M 1993 *Fundamentals of Statistical Signal Processing: Estimation Theory* (Prentice Hall)

[59] Nielsen M A and Chuang I L 2000 *Quantum Computing and Quantum Information* (Cambridge University Press)

[60] Bengtsson I and Zyczkowski K 2006 *Geometry of quantum states: an introduction to quantum entanglement* (Cambridge Univeristy Press)

[61] Helstrom C W 1976 *Quantum detection and estimation theory* (Academic Press)

[62] Holevo A S 1982 *Probabilistic and Statistical Aspects of Quantum Theory* (North Holland)

[63] Braunstein S L and Caves C M 1994 *Phys. Rev. Lett.* **72** 3439–3443

[64] Nagaoka H 2005 *On Fisher Information of Quantum Statistical Models* (World) chap 9, pp 113–125

[65] Toth G and Petz D 2011 *ArXiv e-prints* 1109.2831

[66] Yu S 2013 *ArXiv e-prints* 1302.5311

[67] Fujiwara A 1994 *Math. Eng. Tech. Rep.* **94** 9

[68] Genoni M G, Paris M G A, Adesso G, Nha H, Knight P L, and Kim M S 2012 *ArXiv e-prints* 1206.4867

[69] Fujiwara A 2001 *Phys. Rev. A* **63** 042304

[70] Braunstein S L, Caves C M and Milburn G 1996 *Ann. Phys.* **247** 135 – 173

[71] Aharonov Y, Massar S and Popescu S 2002 *Phys. Rev. A* **66** 2002

[72] Ulam-Orgikh D and Kitagawa M 2001 *Phys. Rev. A* **64** 052106

[73] Caves C M 1981 *Phys. Rev. D* **23** 1693–1708

[74] Monras A and Paris M G A 2007 *Phys. Rev. Lett.* **98** 160401

[75] Adesso G, Dell'Anno F, Siena S D, Illuminati F and Souza L A M 2009 *Phys. Rev. A* **79** 040305(R)

[76] Crowley P J D, Datta A, Barbieri M and Walmsley I A 2012 *ArXiv e-prints* 1206.0043

[77] Hotta M, Karasawa T and Ozawa M 2006 *J. Phys. A: Math. Gen.* **39** 14465

[78] Fujiwara A and Imai H 2003 *J. Phys. A: Math. Gen.* **36** 8093–8103

[79] Fujiwara A 2004 *Phys. Rev. A* **70** 012317

[80] Frey M, Collins D and Gerlach K 2011 *J. Phys. A: Math. Theor.* **44** 205306

[81] Hyllus P, Pezzé L and Smerzi A 2010 *Phys. Rev. Lett.* **105**(12) 120501

[82] Hofmann H F 2009 *Phys. Rev. A* **79** 033822

[83] Zwierz M, Pérez-Delgado C A and Kok P 2010 *Phys. Rev. Lett.* **105** 180402

[84] Anisimov P M, Raterman G M, Chiruvelli A, Plick W N, Huver S D, Lee H and Dowling J P 2010 *Phys. Rev. Lett.* **104** 103602

[85] Giovannetti V and Maccone L 2012 *Phys. Rev. Lett.* **108** 210404

[86] Demkowicz-Dobrzański R, Banaszek K and Schnabel R 2013 *In preparation*

[87] Pezzé L and Smerzi A 2008 *Phys. Rev. Lett.* **100** 073601

[88] Kahn J and Guţă M 2009 *Comm. Math. Phys.* **289** 597–652

[89] Chiribella G, D'Ariano G M and Sacchi M F 2005 *Phys. Rev. A* **72** 042338

[90] Boixo S and Somma R D 2008 *Phys. Rev. A* **77** 052320

[91] Teklu B, Olivares S and Paris M G A 2009 *J. Phys. B: At., Mol. Opt. Phys.* **42** 035502

[92] Demkowicz-Dobrzański R 2011 *Phys. Rev. A* **83** 061802(R)

[93] Hall M J W and Wiseman H M 2012 *New J. Phys.* **14** 033040

[94] Nair R 2012 *ArXiv e-prints* 1204.3761

[95] Grant M and Boyd S 2012 Cvx: Matlab software for disciplined convex programming URL `http://cvxr.com/cvx/`